Spatial-Temporal Modeling of Forest Gaps Generated by Colonization From Below- and Above-Ground Bark Beetle Species

Jun ZHU, Jakob G. RASMUSSEN, Jesper MØLLER, Brian H. AUKEMA, and Kenneth F. RAFFA

Studies of forest declines are important, because they both reduce timber production and affect successional trajectories of landscapes and ecosystems. Of particular interest is the decline of red pines, which is characterized by expanding areas of dead and chlorotic trees in plantations throughout the Great Lakes region. Here we examine the impact of two bark beetle groups, red turpentine beetles and pine engraver bark beetles, on tree mortality and the subsequent gap formation over time in a plantation in Wisconsin. We construct spatial-temporal statistical models that quantify the relations among red turpentine beetle colonization, pine engraver bark beetle colonization, and mortality of red pine trees while accounting for correlation across space and over time. We extend traditional Markov random-field models to include temporal terms and multiple-response variables aimed at developing a suitable set of statistical models for addressing the scientific questions about the forest ecosystem under study. For statistical inference, we adopt a Bayesian hierarchical modeling approach and devise Markov chain Monte Carlo algorithms for obtaining the posterior distributions of model parameters as well as posterior predictive distributions. In particular, we implement path sampling combined with perfect simulation for autologistic models while formally addressing the posterior propriety under an improper uniform prior. Our data analysis results suggest that red turpentine beetle colonization is associated with a higher likelihood of pine engraver bark beetle colonization and that pine engraver bark beetle colonization is associated with higher likelihood of red pine tree mortality, whereas there is no direct association between red turpentine beetle colonization and red pine tree mortality. There is strong evidence that red turpentine beetle colonization does not kill a red pine tree directly, but rather predisposes the tree to subsequent colonization by pine engraver bark beetles. The evidence is also strong that pine engraver bark beetles are the ultimate mortality agents of red pine trees.

KEY WORDS: Autologistic model; Bayesian inference; Forest entomology; Markov chain Monte Carlo; Perfect simulation; Spatial-temporal processes.

1. INTRODUCTION

Studies of forest declines are of great interest to the timber industry, natural resource managers, and ecologists alike, because these declines both reduce timber production and affect successional trajectories of landscapes and ecosystems. Declines are typified by a progressive and chronic deterioration of forest health, as opposed to singular episodes, and typically arise from complex interactions among multiple agents rather than single causes. Decline syndromes occur in forests throughout the world at various scales (Auclair 2005). Declines due to soil acidification and atmospheric pollution may affect large areas (Battles and Fahey 2000; Drohan 2000; Purdon et al. 2004), whereas declines due to insect and/or disease complexes may exhibit smaller mosaics of mortality, such as gap formation, which is our focus here (Klepzig, Raffa, and Smalley 1991; Erbilgin and Raffa 2003). Gaps consist of regions within mature forests in which tree mortality occurs in a highly aggregated fashion. In some systems, areas of large-scale mortality due to insects and pathogens may originate from such small-scale mosaics. Characterizing spatial patterns and gaining inference about the processes that may create such patterns may assist in policy and management decisions when dealing with declines. Indeed, linking pattern and process is a key goal in ecology.

In particular, we examine tree mortality and the subsequent gap formation over time in red pine forests. Decline of red pines is characterized by expanding areas, termed "pockets," of dead, slow-growing, chlorotic trees in plantations throughout the Great Lakes region (Klepzig et al. 1991). Abiotic factors, such as soil characteristics and drought stress, can predispose trees to biotic mortality agents, such as insects and root pathogens (Klepzig et al. 1991; Erbilgin and Raffa 2002). Here we focus on the impact of two bark beetle groups, called "turpentine beetles" and "*Ips* spp.," on the decline of red pines in a plantation in Wisconsin. Details on these species are presented in Section 2.

Past studies on red pine decline have yielded valuable insights into individual components of this system by examining multiple levels of scale, from detailed studies on individual trees (Klepzig, Kruger, Smalley, and Raffa 1995; Raffa and Smalley 1995; Klepzig, Smalley, and Raffa 1996) to regional studies comparing multiple sites (Klepzig et al. 1991; Erbilgin and Raffa 2002, 2003). Despite these advances, however, elucidation of exact mechanisms of pocket development and expansion remain elusive, because a single site has never been observed over more than 3 years. In the present study we examined a 7-year data set of annual surveys of all trees in a plantation. Each year, each of the 2,715 trees was examined for presence/absence of *Ips* spp., tree condition (alive/dead), and number of pitch tubes, each of which signifies colonization by a turpentine beetle. We attempt to answer several important ecological questions. Of greatest interest is how the mortality rate

Jun Zhu is Associate Professor, Department of Statistics, University of Wisconsin–Madison, Madison, WI 53706 (E-mail: *jzhu@stat.wisc.edu*). Jakob G. Rasmussen is Post Doctor (E-mail: *jgr@math.aau.dk*) and Jesper Møller is Professor (E-mail: *jm@math.aau.dk*), Department of Mathematical Sciences, Aalborg University, Aalborg 9220, Denmark. Brian H. Aukema is Research Scientist and Assistant Professor (Adjunct), Canadian Forest Service, Natural Resources Canada at University of Northern British Columbia, Prince George, British Columbia, V2N 4Z9, Canada (E-mail: *baukema@pfc.cfs.nrcan.gc.ca*). Kenneth F. Raffa is Professor, Department of Entomology, University of Wisconsin–Madison, Madison, WI 53706 (E-mail: *raffa@entomology.wisc.edu*). Funding has been provided for this research from National Science Foundation grant DEB-0314215, U.S. Department of Agriculture Hatch grant WIS01096, the Wisconsin Alumni Research Foundation, and Danish Natural Science Research Council grant 272-06-0442, "Point Process Modeling and Statistical Inference." The authors thank the Wisconsin Department of Natural Resources for providing the research site, and the editor, an associate editor, and two referees for constructive and helpful comments.

Journal of the American Statistical Association
March 2008, Vol. 103, No. 481, Applications and Case Studies
DOI 10.1198/016214507000000842

of a tree is associated with the turpentine beetle and *Ips* spp. colonization. For example, how different are the mortality rates between a tree that has been colonized by both groups and a tree that has been colonized by just one group of bark beetles? Related to these questions is the degree of association between turpentine beetle and *Ips* spp. For example, what is the likelihood that a tree colonized by turpentine beetles will be subsequently colonized by *Ips* spp.? Moreover, it is also of interest to quantify the spatial and temporal relations among turpentine beetle colonization, *Ips* spp. colonization, and tree mortality.

The study of red pine declines poses statistical challenges, in that processes giving rise to patterns of mortality may act at different levels of temporal and spatial scales. Here we construct spatial-temporal models that quantify the relationships among the activities of turpentine beetles, the activities of *Ips* spp., and the conditions of red pine trees. Furthermore, we introduce spatial and temporal terms into the model that account for correlations across space and over time. Our chief modeling strategy (and challenge) is to use and extend some of the well-established statistical methodologies and simultaneously develop a suitable set of statistical models for the particular forest ecosystem under study, with the purpose of adequately addressing the scientific questions of interest.

Because our study features discrete spatial-temporal data, there are two principal modeling approaches in the literature that can be considered. One of these approaches, spatial generalized linear mixed models (GLMM), extending from Diggle, Tawn, and Moyeed (1998), concerns atemporal geostatistical data. The response variable is modeled by a probability distribution in the exponential family, conditional on a spatial-temporal random effect typically modeled by a Gaussian process that captures potential spatial and temporal dependence through autocorrelation that decays in spatial and temporal lags. An alternative approach is Markov random field (MRF) models, extending from Besag (1974), which concern atemporal lattice data. The response variable at one spatial location is modeled through a probability distribution conditional on neighboring locations, giving rise to a valid joint distribution at all locations on the lattice under mild regularity conditions. Zhu, Huang, and Wu (2005) extended autologistic models to a general class of spatial-temporal autologistic regression models for the analysis of repeated measures of binary data on a lattice. Because we have a lattice data set with an annual census over a relatively small number of years, we view MRF models as the more appropriate approach and specify spatial-temporal dependence through conditional models in both space and time.

In addition, most MRF models for discrete data concern a single response variable (i.e., univariate). Our study includes three response variables of interest, which calls for a multivariate modeling approach. To incorporate multiple response variables simultaneously, one emerging approach for discrete multivariate spatial data is generalized linear latent variable models (GLLVMs), which can be thought of as factor analysis but with the factors potentially correlated across space. For example, Wang and Wall (2003) and Hogan and Tchernis (2004) proposed a common factor model for atemporal spatial multivariate count data. But the objectives of such multivariate models are focused on inferring the relationships among response variables implicitly through inferring the relationships between response variables and the latent factors, as well as the relationships among the factors. In addition, it is often of interest to optimally map the unobservable factors. In contrast, our primary modeling objective was to explicitly examine the relationships among two bark beetle groups and their relationships to the condition of red pine trees. Therefore, we tailor-made a set of models in such a way that each individual model was a univariate spatial-temporal MRF for a particular response variable and the individual models were linked according to the sequence of all of the response variables over time, an approach that could be of general use and considerable interest in studying insect–tree interactions in other forest ecosystems.

For statistical inference, we adopt a Bayesian hierarchical model and Markov chain Monte Carlo (MCMC) algorithms that enable us to obtain the posterior distributions of the model parameters and posterior predictive distributions. A specific challenge arises in an autologistic model for *Ips* spp. that involves an unknown normalizing constant in the likelihood function. Because direct maximization of the likelihood function is not straightforward, maximum pseudolikelihood estimation (MPLE) has been used (Besag 1975; Gumpertz, Graham, and Ristaino 1997; Zhu et al. 2005). Although MPLE is consistent and asymptotically normal (Guyon 1995), its efficiency depends on the strength of the spatial dependence, and it can be very inefficient when there is strong spatial dependence. Huffer and Wu (1998) proposed using Markov chain Monte Carlo (MCMC) to approximate the normalizing constant and obtain maximum likelihood estimates (MLEs). Their MCMC algorithm relies on an importance sampling scheme developed in earlier work by Geyer and Thompson (1992) that involves a Gibbs sampler to generate Monte Carlo samples from the probability distribution that has an unknown normalizing constant.

Here, in the Bayesian inference context, we adopt a similar approach to approximate a ratio of normalizing constants when computing the Hastings ratio in a Metropolis–Hastings (MH) algorithm. Our MCMC algorithm improves on the previous work in two ways. Instead of importance sampling, we use path sampling, as described by Gelman and Meng (1998), which appears to be more computationally stable. In addition, instead of a Gibbs sampler, we use a relatively new technique known as the Propp–Wilson algorithm for perfect simulation (Propp and Wilson 1996; Møller 1999), which generates exact iid Monte Carlo samples from the probability distribution despite the unknown normalizing constant. We discuss path sampling combined with perfect simulation in more detail in Section 4.

Furthermore, within the Bayesian hierarchical modeling framework, we use a technique proposed by Gelman, Meng, and Stern (1996) to assess model fitting by examining the discrepancies between observed and posterior predictive values. This assessment provides a systematic way to examine various aspects of model fitting. For our study, we are particularly interested in how well the relationships among the multiple response variables and the spatial-temporal patterns are represented. We also use this technique to compare our more complicated spatial-temporal models with some simpler models.

Finally, we investigate the propriety of posteriors under improper uniform priors. To the best of our knowledge, this issue has not been addressed formally for MRF models with an unknown normalizing constant in the likelihood function. The most relevant work that we could find is work by Foster (2006) that concerns Bayesian inference for independent Poisson variables. Thus we expect the result to be of value to Bayesian inference on MRF models in general.

The remainder of the article is organized as follows. In Section 2 we describe the data and provide more ecological details. In Section 3 we specify a set of spatial-temporal models for the data. We specify the Bayesian model and simulation algorithms in Section 4 and describe the results of the data analysis and address the ecological questions in Section 5. In Section 6 we present concluding remarks.

2. BARK BEETLE AND RED PINE DATA

2.1 Background

Bark beetle species are characterized by their ability to mine and reproduce below the surface of the bark of trees. The red turpentine beetle [*Dendroctonus valens* (LeConte)], also known as the "turpentine beetle," is one of the most widely distributed bark beetles in North America. Colonization by turpentine beetle adults is concentrated in the lower stems of pine trees. The larvae breed largely below the soil line in the root collar and primary lateral root regions. An external indicator of colonization by the turpentine beetle is a pitch tube on the outer surface of the bark just above the soil line or pitch pellets on the ground. Peak flight and colonization in Wisconsin occur in late April and May. Turpentine beetles colonize primarily trees that are weakened by drought and fire, for example, but may also colonize apparently healthy trees. These beetles vector the staining fungi *Leptographium terebrantis* and *L. procerum* (Klepzig et al. 1991), which do not kill mature trees, but do weaken their overall condition. It is hypothesized that a colonization of a healthy tree by turpentine beetles does not kill the tree but may predispose it to subsequent colonization by other bark beetles such as engraver beetles.

Engraver beetles [predominantly *Ips pini* (Say), with some *Ips grandicollis* (Eichhoff) in our study site (Klepzig et al. 1991)], which we call "*Ips* spp.," may have up to three generations from spring to early fall (Erbilgin, Nordheim, Aukema, and Raffa 2002; Erbilgin and Raffa 2002; Aukema, Clayton, and Raffa 2005). Successful colonization by *Ips* spp. is indicated by fine sawdust shavings pushed to the outer surface of the bark and galleries inside the tree. *Ips* spp. beetles produce aggregation pheromones as they enter host trees, thus attacking trees en masse over very short periods. These mass attacks typically result in complete utilization of the resource (i.e., the thin layer of phloem tissue beneath the bark) within a single generation, making it unlikely that subsequent *Ips* spp. or turpentine beetles will enter. *Ips* spp. also vector the fungal associate *Ophiostoma ips*, the colonization of which may impede the upward flow of water to the tree crowns. Lack of water leads the needles to wither and die while the color characteristically fades from green to red to brown. *Ips* spp. brood adults leave the tree through emergence holes on the surface of the outer bark, the most apparent external indicator that a tree has been colonized by *Ips* spp. The tree is most likely to die within a few weeks after an attack.

2.2 Description of Data

The study area is a red pine plantation near Spring Green, Wisconsin. On this plantation, the red pine trees were planted on a regular 1.82×1.82 m (i.e., 6×6 ft) grid. In 1986, each of the 2,715 trees in the plantation was surveyed and its condition (alive/dead) recorded. From 1987 to 1992, subsequent surveys were conducted both of tree condition and of the colonization of turpentine beetles and *Ips* spp. For turpentine beetles, the number of pitch tubes on the outer surface of a bark was recorded, whereas for *Ips* spp., an indicator variable of *Ips* spp. colonization (yes/no) was recorded. The survey was done in autumn of each year, after beetles had become dormant.

Selected image plots in Figure 1 illustrate the nature of the data. For 1987, colonization of turpentine beetles (zero or positive number of pitch tubes), colonization of *Ips* spp. (yes/no), and condition of trees (alive/dead) are shown [Figs. 1(a)–1(c)]. For 1992, similar plots are shown, except that colonization of *Ips* spp. here includes colonization from 1987 to 1992 [Figs. 1(d)–1(f)]. There is clear indication of spatial dependence among tree conditions, *Ips* spp. colonization, and turpentine beetle colonization. A gap of dead trees was evident in the southeastern part of the plantation in the beginning, and this gap expanded over the years. Furthermore, there was a strong association between the spatial pattern of *Ips* spp. colonization and that of tree mortality, but the link between turpentine beetle colonization and tree mortality was not as obvious.

There were 126 dead trees in 1986. Between 1987 and 1992, a total of 344 trees died, 339 trees were colonized by *Ips* spp., and 152 trees were colonized by turpentine beetles. Among the 344 dead trees, 330 were colonized by *Ips* spp. and 73 were colonized by turpentine beetles. Only 9 of the 339 trees colonized by *Ips* spp. survived to 1992, whereas 79 of the 152 of the trees colonized by turpentine beetles survived. *Ips* spp. colonization seemed to be more associated with those trees with a larger number of pitch tubes of turpentine beetles, although the evidence of this was subtle, due to the small number of trees with a large number of pitch tubes.

3. OBSERVATION MODEL

3.1 Notation

Let $t = -1, 0, \ldots, 5$ index the time of survey from 1986 to 1992, and let $i = 1, \ldots, 2{,}715$ index the sites of 2,715 red pine trees in the plantation that were surveyed. For the purpose of modeling, we consider time points $t = \ldots, -1, 0, 1, \ldots$ and define $x_{t,i}$, $y_{t,i}$, $z_{t,i}$, and $u_{t,i}$ as follows. Because the survey was conducted in autumn, after insect and tree dormancy for any given year, the data reflect insect activity and tree conditions throughout that year. At time t and site i, let $x_{t,i}$ denote the turpentine beetle colonization variable such that

$$x_{t,i} = \text{the cumulative number of turpentine beetle pitch tubes on the bark.}$$

Furthermore, let $y_{t,i}$ denote the *Ips* spp. colonization variable such that

$$y_{t,i} = \begin{cases} 0, & \text{no } \textit{Ips} \text{ spp. colonization by time } t \text{ and site } i \\ 1, & \text{colonization by } \textit{Ips} \text{ spp. in year } t \text{ and site } i \\ 2, & \text{colonization by } \textit{Ips} \text{ spp. by year } t-1 \text{ and site } i. \end{cases}$$

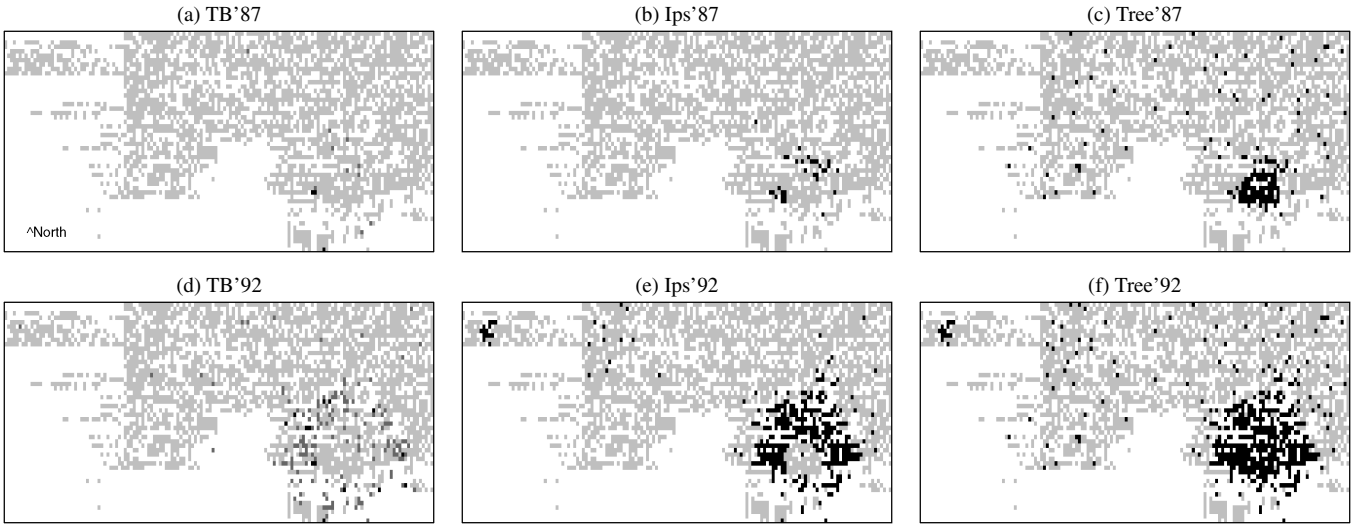

Figure 1. (a) and (d) Turpentine beetle (TB) colonization; (b) and (e) *Ips* spp. colonization; (c) and (f) tree condition by 1987 (top row) and 1992 (bottom row). The site of a tree is dark-gray if the number of turpentine beetle pitch tubes is between 1 and 4 and black if more than 4 [(a) and (d)]. Similarly, the site of a tree is black if the tree was colonized by *Ips* spp. [(b) and (e)] or dead [(c) and (f)]; all other sites are light-gray.

Let $u_{t,i}$ denote an indicator variable of whether *Ips* spp. colonization occurred during year t at site i, that is,

$$u_{t,i} = \begin{cases} 1, & y_{t,i} = 1 \\ 0, & y_{t,i} = 0 \text{ or } 2. \end{cases}$$

Consistent with scientific understanding of the system, we assume that *Ips* spp. colonization could occur only once at a given site and after colonization of a tree, *Ips* spp. leaves the tree before the end of the flight season of the same year (before the annual survey). Thus $u_{t,i} = 1$ for at most one year t. Finally, let $z_{t,i}$ denote the tree condition variable such that

$$z_{t,i} = \begin{cases} 0, & \text{tree was alive at time } t \text{ and site } i \\ 1, & \text{tree was dead at time } t \text{ and site } i. \end{cases}$$

Let $\mathbf{x}_t = (x_{t,1}, \ldots, x_{t,2715})$, $\mathbf{y}_t = (y_{t,1}, \ldots, y_{t,2715})$, and $\mathbf{z}_t = (z_{t,1}, \ldots, z_{t,2715})$ denote the vectors of the turpentine beetle colonization variables, the *Ips* spp. colonization variables, and the tree condition variables at time t and all the sites. Furthermore, let $\mathbf{w}_t = (\mathbf{x}_t, \mathbf{y}_t, \mathbf{z}_t)$. Because turpentine beetle colonization typically precedes *Ips* spp. colonization, which in turn precedes the death of a tree, we order the variables $\mathbf{x}_t, \mathbf{y}_t$, and $\mathbf{z}_t$ such that $\mathbf{x}_t$ precedes $\mathbf{y}_t$ and $\mathbf{y}_t$ precedes $\mathbf{z}_t$. Thus the data under study are ordered as $(\mathbf{z}_{-1}, \mathbf{x}_0, \mathbf{y}_0, \mathbf{z}_0, \ldots, \mathbf{x}_5, \mathbf{y}_5, \mathbf{z}_5)$, whereas the unobserved past data are ordered as $(\ldots, \mathbf{x}_{-2}, \mathbf{y}_{-2}, \mathbf{z}_{-2}, \mathbf{x}_{-1}, \mathbf{y}_{-1})$.

3.2 Temporal Model

In Sections 3.3–3.5 we construct a set of spatial-temporal models to capture the relationships among the variables $x_{t,i}$, $y_{t,i}$, and $z_{t,i}$ while accounting for spatial and temporal dependence. Before specifying these details, it is useful to give a brief description of the temporal process $\mathbf{w}_t$ and how the likelihood factorizes.

In (1)–(3) we naturally consider a sequential model construction such that for each time t, we specify the conditional distribution of $\mathbf{x}_t$ first, $\mathbf{y}_t$ second, and $\mathbf{z}_t$ third given the relevant past. The detailed model descriptions (7), (10), and (14) in Sections 3.3–3.5 imply the following conditional independence structure for the temporal process. Let $[a|b]$ denote the conditional distribution of a random component a given another random component b. For the turpentine beetle colonization variables at time t,

$$[\mathbf{x}_t | (\mathbf{w}_s)_{s=t-1,t-2,\ldots}] \sim [\mathbf{x}_t | \mathbf{x}_{t-1}, \mathbf{z}_{t-1}] \tag{1}$$

depends on a parameter $\boldsymbol{\theta}$ as specified in Section 3.3; for the *Ips* spp. beetle colonization variables at time t,

$$[\mathbf{y}_t | \mathbf{x}_t, (\mathbf{w}_s)_{s=t-1,t-2,\ldots}] \sim [\mathbf{y}_t | \mathbf{x}_t, \mathbf{y}_{t-1}, \mathbf{z}_{t-1}] \tag{2}$$

depends on a parameter $\boldsymbol{\psi}$ (Sec. 3.4); for the tree condition variables at time t,

$$[\mathbf{z}_t | \mathbf{x}_t, \mathbf{y}_t, (\mathbf{w}_s)_{s=t-1,t-2,\ldots}] \sim [\mathbf{z}_t | \mathbf{x}_t, \mathbf{y}_t, \mathbf{z}_{t-1}] \tag{3}$$

depends on a parameter $\boldsymbol{\varphi}$ (Sec. 3.5). For the corresponding likelihood terms, we write $L_t^{(1)}(\boldsymbol{\theta}) = L^{(1)}(\boldsymbol{\theta}; \mathbf{x}_t | \mathbf{x}_{t-1}, \mathbf{z}_{t-1})$, $L_t^{(2)}(\boldsymbol{\psi}) = L^{(2)}(\boldsymbol{\psi}; \mathbf{y}_t | \mathbf{x}_t, \mathbf{y}_{t-1}, \mathbf{z}_{t-1})$, and $L_t^{(3)}(\boldsymbol{\varphi}) = L^{(3)}(\boldsymbol{\varphi}; \mathbf{z}_t | \mathbf{x}_t, \mathbf{y}_t, \mathbf{z}_{t-1})$.

For statistical inference, we condition on

$$\mathbf{e} = (\mathbf{z}_{-1}, \mathbf{x}_0, \mathbf{y}_0), \tag{4}$$

because, by (1)–(3), the remaining data,

$$\mathbf{d} = (\mathbf{z}_0, \mathbf{x}_1, \mathbf{y}_1, \mathbf{z}_1, \ldots, \mathbf{x}_5, \mathbf{y}_5, \mathbf{z}_5), \tag{5}$$

are conditionally independent of the unobserved $(\ldots, \mathbf{x}_{-2}, \mathbf{y}_{-2}, \mathbf{z}_{-2}, \mathbf{x}_{-1}, \mathbf{y}_{-1})$. We let $L(\boldsymbol{\theta}, \boldsymbol{\psi}, \boldsymbol{\varphi}) = L(\boldsymbol{\theta}, \boldsymbol{\psi}, \boldsymbol{\varphi}; \mathbf{d}|\mathbf{e})$ denote the likelihood based on the conditional distribution of $\mathbf{d}$ given $\mathbf{e}$. By (1)–(3), this factorizes to

$$L(\boldsymbol{\theta}, \boldsymbol{\psi}, \boldsymbol{\varphi}; \mathbf{d}|\mathbf{e}) = L^{(1)}(\boldsymbol{\theta}) L^{(2)}(\boldsymbol{\psi}) L^{(3)}(\boldsymbol{\varphi}),$$

given by the likelihood terms for each type of data,

$$L^{(1)}(\boldsymbol{\theta}) = \prod_{t=1}^{5} L_t^{(1)}(\boldsymbol{\theta}),$$

$$L^{(2)}(\boldsymbol{\varphi}) = \prod_{t=1}^{5} L_t^{(2)}(\boldsymbol{\varphi}), \qquad \text{and} \tag{6}$$

$$L^{(3)}(\boldsymbol{\psi}) = \prod_{t=0}^{5} L_t^{(3)}(\boldsymbol{\psi}),$$

where $L_t^{(1)}(\boldsymbol{\theta}) = L^{(1)}(\boldsymbol{\theta}; \mathbf{x}_t|\mathbf{x}_{t-1}, \mathbf{z}_{t-1})$, $L_t^{(2)}(\boldsymbol{\psi}) = L^{(2)}(\boldsymbol{\psi}; \mathbf{y}_t|\mathbf{x}_t, \mathbf{y}_{t-1}, \mathbf{z}_{t-1})$, and $L_t^{(3)}(\boldsymbol{\varphi}) = L^{(3)}(\boldsymbol{\varphi}; \mathbf{z}_t|\mathbf{x}_t, \mathbf{y}_t, \mathbf{z}_{t-1})$ are as specified at the end of Sections 3.3–3.5.

In Sections 3.3–3.5 our strategy is for each time, site, and type of data, $x_{t,i}$, $y_{t,i}$, or $z_{t,i}$, to specify a "local characteristic" that depends only on "local information." For example, by the local characteristic of $y_{t,i}$, we mean the conditional distribution of $y_{t,i}$ given the other $y_{t,j}$, $j \neq i$, and the previous history $\mathbf{x}_t$, $(\mathbf{w}_s)_{s=t-1,t-2,\ldots}$. We express the local information with respect to the grid of tree locations and consider for site i its first-, second-, third-, fourth-, and fifth-order neighbors, which are the (up to) four nearest, four second-nearest, four third-nearest, four fourth-nearest, and four fifth-nearest sites to site i of a focal tree, corresponding to 1.82, 2.54, 3.64, 4.07, and 5.14 m in physical distance.

3.3 Likelihood Based on Turpentine Beetle Colonization

The cumulative number of turpentine beetles at time t and site i is assumed to depend on local information such that

$$[x_{t,i}|(x_{t,j})_{j\neq i}, (\mathbf{w}_s)_{s=t-1,t-2,\ldots}] \sim \left[x_{t,i}|\mathbf{x}_{t-1,N_i^x}, z_{t-1,i}\right], \tag{7}$$

where $\mathbf{x}_{t-1,N_i^x}$ is the vector of variables $x_{t-1,j}$ with $j \in N_i^x$. Here N_i^x consists of i and its neighbors up to the fifth order, and we assume that the conditional distribution of turpentine beetle colonization at time t depends only on turpentine beetle colonization at time $t-1$ and at sites in N_i^x, because this neighborhood is fairly large but is still interpretable biologically (see Sec. 5 for more details). Because turpentine beetles colonize red pines during only one brief period per year, and a tree can be colonized by multiple turpentine beetles, we assume conditional independence among nearby sites within the same year. On the other hand, turpentine beetles that colonize a tree in one spring tend to colonize nearby trees in the next spring. Thus we build into the model a possible relationship between turpentine beetle colonization at time t and at time $t-1$.

The local characteristic $[x_{t,i}|\mathbf{x}_{t-1,N_i^x}, z_{t-1,i}]$ is specified as follows. If the tree at site i was dead at time $t-1$ (i.e., $z_{t-1,i} = 1$), then the local characteristic is deterministic with $x_{t,i} = x_{t-1,i}$, because turpentine beetles will not colonize a dead tree. Turpentine beetles could theoretically colonize a tree that dies from competitive thinning, that is, a process in which the growth of neighboring trees blocks out necessary sunlight. However, such events were rare in the stand, because the insects would likely colonize the weakened tree in advance of tree death. Moreover, the diameter and subcortical tissues of trees that have been crowded to death are frequently too thin to serve as a suitable breeding substrate for this insect. Turpentine beetles also could colonize a healthy tree that was killed suddenly, such as by a lightning strike or during a wind storm. But we did not find any visual evidence of lightning (e.g., shredded bark, burn marks, or shattered limbs) or windthrow (other than trees that had already been killed) in any of our annual surveys. Thus, focusing on the colonization of live trees, if the tree at site i was alive at time $t-1$ (i.e., $z_{t-1,i} = 0$), then we assume that the conditional distribution of the number of turpentine beetles at time t is given by

$$\left[x_{t,i} - x_{t-1,i}|\mathbf{x}_{t-1,N_i^x}, z_{t-1,i} = 0\right] \sim \text{Poisson}(\lambda_{t,i}),$$

where

$$\log(\lambda_{t,i}) = \theta_0 + \theta_1 \sum_{j\in N_i^x} x_{t-1,j}. \tag{8}$$

Thus, given the past, the $x_{t,i} - x_{t-1,i}$ with $z_{t-1,i} = 0$ form a sample from a Poisson regression, so

$$\begin{aligned} L_t^{(1)}(\boldsymbol{\theta}) &\propto \prod_{i:z_{t-1,i}=0} \lambda_{t,i}^{x_{t,i}-x_{t-1,i}} \exp(-\lambda_{t,i}) \\ &= \exp\Bigg[\sum_{i:z_{t-1,i}=0} \Bigg\{(x_{t,i} - x_{t-1,i})\Bigg(\theta_0 + \theta_1 \sum_{j\in N_i^x} x_{t-1,j}\Bigg) \\ &\qquad - \exp\Bigg(\theta_0 + \theta_1 \sum_{j\in N_i^x} x_{t-1,j}\Bigg)\Bigg\}\Bigg]. \end{aligned} \tag{9}$$

3.4 Likelihood Based on *Ips* spp. Colonization

The conditional dependence structure for whether colonization by *Ips* beetles has occurred is assumed to be

$$\begin{aligned} &[y_{t,i}|\mathbf{x}_t, (y_{t,j})_{j\neq i}, (\mathbf{w}_s)_{s=t-1,t-2,\ldots}] \\ &\qquad \sim \left[y_{t,i}|x_{t,i}, \mathbf{u}_{t,N_i^y}, \mathbf{u}_{t-1,N_i^y}, y_{t-1,i}, z_{t-1,i}\right]. \end{aligned} \tag{10}$$

Thus we assume that the conditional distribution of *Ips* spp. colonization at time t depends on turpentine beetle colonization at time t and on *Ips* spp. colonization at sites $j \in N_i^y$ at times $t-1$ and t, where N_i^y comprises the first- and second-order neighbors to i (note that N_i^y does not include i). Because it is hypothesized that turpentine beetles predispose red pines to colonization by *Ips* spp., we include in the model a possible relationship to the number of turpentine beetle pitch tubes on the tree. Because *Ips* spp. attack different red pines one to three times per year and can overwinter near the trees that they have colonized, we assume relationships among neighboring sites for both time t and $t-1$ and assume that a first- and second-order neighborhood suffices to represent spatial dependence in this study.

The local characteristic $[y_{t,i}|x_{t,i}, \mathbf{u}_{t,N_i^y}, \mathbf{u}_{t-1,N_i^y}, y_{t-1,i}, z_{t-1,i}]$ is specified as follows. If the tree at site i was dead at time $t-1$ (i.e., $z_{t-1,i} = 1$) or was colonized by *Ips* spp. at previous times (i.e., $y_{t-1,i} = 1$ or 2), then the local characteristic is deterministic with $y_{t,i} = 0$ or 2, because *Ips* spp. will not colonize a dead tree. *Ips* spp. could theoretically colonize a tree that dies from competitive thinning (i.e., overshadowing and crowding by more dominant neighbors), although in practice the insects likely would find and colonize a weakened tree in advance of tree death and would colonize only if the subcortical tissue were sufficiently thick. Such trees also contribute

little to the ecological dynamics of the system, because they are commonly colonized by competing species of insects against which *Ips* spp. fare poorly. We also disregard the possibility that *Ips* spp. colonize lightning strikes or recent windthrow of live trees, due to the absence of such events observed during our annual surveys. Thus focusing on colonization of live trees, if the tree at site i was alive at time $t-1$ (i.e., $z_{t-1,i}=0$) and was not colonized previously ($y_{t-1,i}=0$), the local characteristic is assumed to be a logistic regression,

$$\left[y_{t,i}|x_{t,i}, \mathbf{u}_{t,N_i^y}, \mathbf{u}_{t-1,N_i^y}, y_{t-1,i}=0, z_{t-1,i}=0\right] \sim \text{Bernoulli}(p_{t,i}), \quad (11)$$

where

$$\text{logit}(p_{t,i}) = \psi_0 + \psi_1 x_{t,i} + \psi_2 \sum_{j\in N_i^y} u_{t-1,j} + \psi_3 \sum_{j\in N_i^y} u_{t,j}. \quad (12)$$

Because $u_{t,i}=y_{t,i}$ in (11), by the Hammersley–Clifford theorem, $L_t^{(2)}(\boldsymbol{\psi})$ is equal to

$$\exp\Bigg(\sum_{i:y_{t-1,i}=z_{t-1,i}=0}\Bigg[\psi_0+\psi_1 x_{t,i}+\psi_2\sum_{j\in N_i^y}u_{t-1,j}\Bigg]u_{t,i} + \psi_3\sum_{i<j:\, j\in N_i^y} u_{t,i}u_{t,j}\Bigg)\Big/ c(\mathbf{x}_t, \mathbf{y}_{t-1}, \mathbf{z}_{t-1}, \boldsymbol{\psi}), \quad (13)$$

where $c(\mathbf{x}_t, \mathbf{y}_{t-1}, \mathbf{z}_{t-1}, \boldsymbol{\psi})$ is a normalizing constant (note that $j\in N_i^y \Leftrightarrow i\in N_j^y$). In other words, given the past, the $u_{t,i}$ with $y_{t,i}=z_{t,i}=0$ form an autologistic model (Besag 1974).

3.5 Likelihood Based on Tree Condition

The conditional dependence structure for tree condition is assumed to be

$$[z_{t,i}|\mathbf{x}_t, \mathbf{y}_t, (z_{t,j})_{j\neq i}, (\mathbf{w}_s)_{s=t-1,t-2,\ldots}] \sim \left[z_{t,i}|x_{t,i}, u_{t,i}, \mathbf{z}_{t-1,N_i^z}, z_{t-1,i}\right], \quad (14)$$

where the neighborhood N_i^z consists of the neighbors up to the fifth order. If the tree at site i was dead at time $t-1$ (i.e., $z_{t-1,i}=1$), then the local characteristic is deterministic with $z_{t,i}=1$, because a dead tree remains dead. But if the tree at site i was alive at time $t-1$ (i.e., $z_{t-1,i}=0$), then the local characteristic is assumed to be a logistic regression,

$$\left[z_{t,i}|x_{t,i}, u_{t,i}, \mathbf{z}_{t-1,N_i^z}, z_{t-1,i}=0\right] \sim \text{Bernoulli}(q_{t,i}),$$

where

$$\text{logit}(q_{t,i}) = \varphi_0 + \varphi_1 x_{t,i} + \varphi_2 u_{t,i} + \varphi_3 \sum_{j\in N_i^z} z_{t-1,j}. \quad (15)$$

That is, mortality rate of a tree depends on both turpentine beetle colonization and *Ips* spp. colonization. The additional term involving the tree condition at time $t-1$ provides a way to account for any potential spatial dependence. Again, we consider a fairly large neighborhood comprising neighbors up to the fifth order. Conditional on the past, the $z_{t,i}$ with $z_{t-1,i}=0$ form a sample from a logistic regression, so that

$$\begin{aligned} L_t^{(3)}(\boldsymbol{\varphi}) &= \prod_{i:z_{t-1,i}=0} \frac{\exp(z_{t,i}\,\text{logit}(q_{t,i}))}{1+\exp(\text{logit}(q_{t,i}))} \\ &= \prod_{i:z_{t-1,i}=0} \exp\Bigg(z_{t,i}\Bigg(\varphi_0+\varphi_1 x_{t,i}+\varphi_2 u_{t,i} + \varphi_3\sum_{j\in N_i^z} z_{t-1,j}\Bigg)\Bigg) \\ &\quad \Big/\Bigg\{1+\exp\Bigg(\varphi_0+\varphi_1 x_{t,i}+\varphi_2 u_{t,i} + \varphi_3\sum_{j\in N_i^z} z_{t-1,j}\Bigg)\Bigg\}. \end{aligned} \quad (16)$$

4. BAYESIAN MODEL AND POSTERIOR SIMULATIONS

We assume independent improper uniform priors

$$p(\boldsymbol{\theta})\propto 1, \quad \boldsymbol{\theta}\in\mathbb{R}^2; \qquad p(\boldsymbol{\psi})\propto 1, \quad \boldsymbol{\psi}\in\mathbb{R}^4; \quad \text{and} \qquad p(\boldsymbol{\varphi})\propto 1, \quad \boldsymbol{\varphi}\in\mathbb{R}^4.$$

Thus $\boldsymbol{\theta}$, $\boldsymbol{\psi}$, and $\boldsymbol{\varphi}$ are a posteriori independent with densities

$$\pi(\boldsymbol{\theta})\propto L^{(1)}(\boldsymbol{\theta}), \quad \boldsymbol{\theta}\in\mathbb{R}^2; \qquad \pi(\boldsymbol{\psi})\propto L^{(2)}(\boldsymbol{\psi}), \quad \boldsymbol{\psi}\in\mathbb{R}^4; \quad \text{and} \qquad \pi(\boldsymbol{\varphi})\propto L^{(3)}(\boldsymbol{\varphi}), \quad \boldsymbol{\varphi}\in\mathbb{R}^4. \quad (17)$$

(For a discussion of posterior propriety, see the App.) For the remaining discussion of MCMC simulations, we assume that the reader is familiar with MCMC methods (e.g., Robert and Casella 2004).

For turpentine beetles, we simulate from the marginal posterior distribution of $\boldsymbol{\theta}$ using a Metropolis-within–Gibbs algorithm, where we alternate between updating θ_0 and θ_1. Because the full conditional for $\lambda_0=\exp(\theta_0)$ is a gamma distribution with shape parameter $\sum_{t,i}(x_{t,i}-x_{t-1,i})$ and inverse scale parameter $\sum_{t,i}\exp(\theta_1\sum_{j\in N_i^x}x_{t-1,j})$, where in both cases the sum $\sum_{t,i}$ is over those t and i with $z_{t-1,i}=y_{t-1,i}=0$, we use a Gibbs update for this component. The full conditional for the other parameter θ_1 is not a standard distribution, so we use a Metropolis random-walk algorithm with a normal proposal distribution (cf. Robert and Casella 2004).

For *Ips* spp., we use a Metropolis–Hastings algorithm to simulate from the marginal posterior distribution of $\boldsymbol{\psi}$. Let $L^{(2)}_{\text{unnorm}}(\boldsymbol{\psi};\mathbf{u})$ denote $L^{(2)}$ in (6) but without the unknown normalizing constant

$$c(\boldsymbol{\psi}) = \prod_{t=1}^{5} c(\mathbf{x}_t, \mathbf{y}_{t-1}, \mathbf{z}_{t-1}, \boldsymbol{\psi})$$

from (13); here $\mathbf{u}$ denotes the vector of all observed $u_{t,i}$ values. If $\boldsymbol{\psi}$ is the current and $\boldsymbol{\psi}'$ the proposed parameter values in the Metropolis–Hastings algorithm, then the Hastings ratio depends on the ratio of unknown normalizing constants,

$c(\boldsymbol{\psi}')/c(\boldsymbol{\psi})$. This can be approximated by path sampling (e.g., Gelman and Meng 1998),

$$\log \frac{c(\boldsymbol{\psi}')}{c(\boldsymbol{\psi})} \approx \frac{1}{n}\sum_{k=1}^{n}\left[\frac{\mathrm{d}}{\mathrm{d}s}\log L^{(2)}_{\mathrm{unnorm}}(\boldsymbol{\psi}(s_k);\boldsymbol{\upsilon}_k)\right]. \quad (18)$$

Here we let $s_1,\ldots,s_n$ be independent and uniformly distributed on [0, 1], and $\boldsymbol{\psi}(s) = s\boldsymbol{\psi}' + (1-s)\boldsymbol{\psi}$, $0 \le s \le 1$, is a line segment. Alternatively, importance sampling could be used to approximate the ratio of normalizing constants in an approach similar to that of Huffer and Wu (1998), who introduced a reference parameter $\boldsymbol{\psi}^*$ for generating Monte Carlo samples. One difference between path sampling and importance sampling is that several parameters along the path from $\boldsymbol{\psi}$ to $\boldsymbol{\psi}'$ are involved rather than a single $\boldsymbol{\psi}^*$. Whereas the amount of computation is larger with path sampling, there appears to be an increased level of stability in computation.

Furthermore, each $\boldsymbol{\upsilon}_k$ is a perfect simulation of $\mathbf{u} = (\mathbf{u}_1,\ldots,\mathbf{u}_5)$, where $\mathbf{u}_t$ given the past follows the autologistic model (13) with parameter $\boldsymbol{\psi}(s_k)$ (Propp and Wilson 1996; Møller 1999). The main idea of perfect simulation is to run two Markov chains, one as an upper bound and the other as a lower bound, starting further back in time until the two chains coalesce. Theory guarantees that the Monte Carlo sample generated in this way is at equilibrium and, in our case, is from the probability distribution of the model for *Ips* spp. exactly despite the unknown normalizing constant $c(\boldsymbol{\psi})$. Given $s_1,\ldots,s_n$, the perfect simulations $\boldsymbol{\upsilon}_1,\ldots,\boldsymbol{\upsilon}_n$ are independent. Indeed, other path sampling approximations based on "conventional" (i.e., nonperfect) MCMC methods exist, but these methods require determination of both an appropriate quadrature rule and an appropriate burn-in for each of several Metropolis–Hastings chains corresponding to different choices of the parameters along the path (Gelman and Meng 1998). Using perfect simulation as described earlier has the advantage of being automatic in the sense that there is no need to make choices of a quadrature rule or a burn-in. Perfect simulation has the added advantage in that, unlike a traditional Gibbs sampler, it does not require subsampling to obtain (nearly) independent samples, because repeated perfect simulation results in iid samples.

We use a Metropolis random-walk algorithm with independent normal proposal distributions for ψ_0, ψ_1, ψ_2, and ψ_3, where we propose to change all four parameters at the same time, because the main part of the running time of the algorithm is used to generate the perfect simulations, which represents the same amount of work whether we are changing one or all four parameters.

For tree condition, we use a Metropolis-within-Gibbs algorithm, in which we alternate simulating from the marginal posterior distributions of $\varphi_0, \varphi_1, \varphi_2$, and φ_3. Neither of these parameters has a standard distributions, so for each parameter we use a Metropolis random-walk update with a normally distributed proposal.

When running the Metropolis random-walk algorithm for either $\theta_1, \boldsymbol{\psi}, \varphi_0, \varphi_1, \varphi_2$, or φ_3, we choose the standard deviation of the normal proposal distribution to reach an average acceptance probability of about .3 (Roberts, Gelman, and Gilks 1997). The starting values for all of the parameters are set at 0, except the maximum pseudolikelihood estimate is used as the starting value for $\boldsymbol{\psi}$. Convergence of the MCMC algorithms is determined by examining trace plots, some of which are shown in Figures 2–4.

In addition, we consider simpler models in which spatial-temporal dependence is unaccounted for, which we call the independence models. The independence models can be reduced from the space–time models by setting $\theta_1 = 0$ for turpentine beetles, $\psi_2 = \psi_3 = 0$ for *Ips* spp., and $\varphi_3 = 0$ for tree condition. Again assuming independent improper uniform priors, we obtain Monte Carlo samples from the posterior distribution using similar MCMC algorithms. In particular, a Gibbs sampler with a gamma full conditional distribution is used to sample θ_0, and a Metropolis-within-Gibbs algorithm is used to update ψ_0 and ψ_1 in the turpentine beetle model and φ_0, φ_1, and φ_2 in the tree condition model in a manner similar to that for $\boldsymbol{\varphi}$ in the spatial-temporal model for tree condition.

5. STATISTICAL INFERENCE AND DISCUSSION OF THE ECOLOGICAL QUESTIONS

5.1 Posterior Distributions of the Model Parameters

For inference of the parameters $\boldsymbol{\theta}$ in the turpentine beetle colonization model, Figures 2(a) and 2(b) give the posterior distributions based on an MCMC run length of 100,000 with a burn-in length of 1,000. The results suggest that there is a positive relationship between the new turpentine beetle colonization and the number of turpentine beetle tubes in the previous year not only at the same site, but also at sites up to fifth-order neighbors. That is, the more turpentine beetles there were in the previous year on a tree and its neighboring trees, the more new colonization can be expected to occur on this tree in the current year. Here the extent of local temporal dependence is represented by a 1-year lag and that of local spatial dependence is represent by about 5.14 m, the distance between a fifth-order neighbor and the site of a tree. We also fitted a model that has one term for the zero-, first-, and second-order neighbors and another term for the third-, fourth-, and fifth-order neighbors. The results (not shown) suggest that the regression coefficients for the two types of neighborhoods are similar, and thus we combine all of the neighbors up to the fifth order. This phenomenon is consistent with a hypothesis in which turpentine beetles colonize trees that are being slowly weakened by the spread of a root fungus, such as *L. terebrantis* or *L. procerum*. These fungi are introduced to trees by the beetles and spread through root grafts at a rate of 5 m per year, according to our best estimates based on root excavations and fungal isolations (Klepzig et al. 1991; Erbilgin and Raffa 2002). This hypothesis is consistent with the work of Erbilgin and Raffa (2003), who found that the probability of tree death falls below 50% at a distance of 5 m from the outer edge of the pocket margin. In comparison, Figure 2(c) gives the posterior distribution of θ_0 under the independence model, which has a larger value for the center and a smaller value for the spread of the distribution.

For inference of the parameters $\boldsymbol{\psi}$ in the *Ips* spp. colonization model, Figures 3(a)–3(d) give the posterior distributions of ψ_0, ψ_1, ψ_2, and ψ_3, based on an MCMC run length of 60,000 with a burn-in length of 1,000. For the approximation (18), we use only $n = 10$ perfect simulations, because some preliminary experiments showed that the approximation of the normalizing constant ratio was effectively the same whether $n = 10$ or

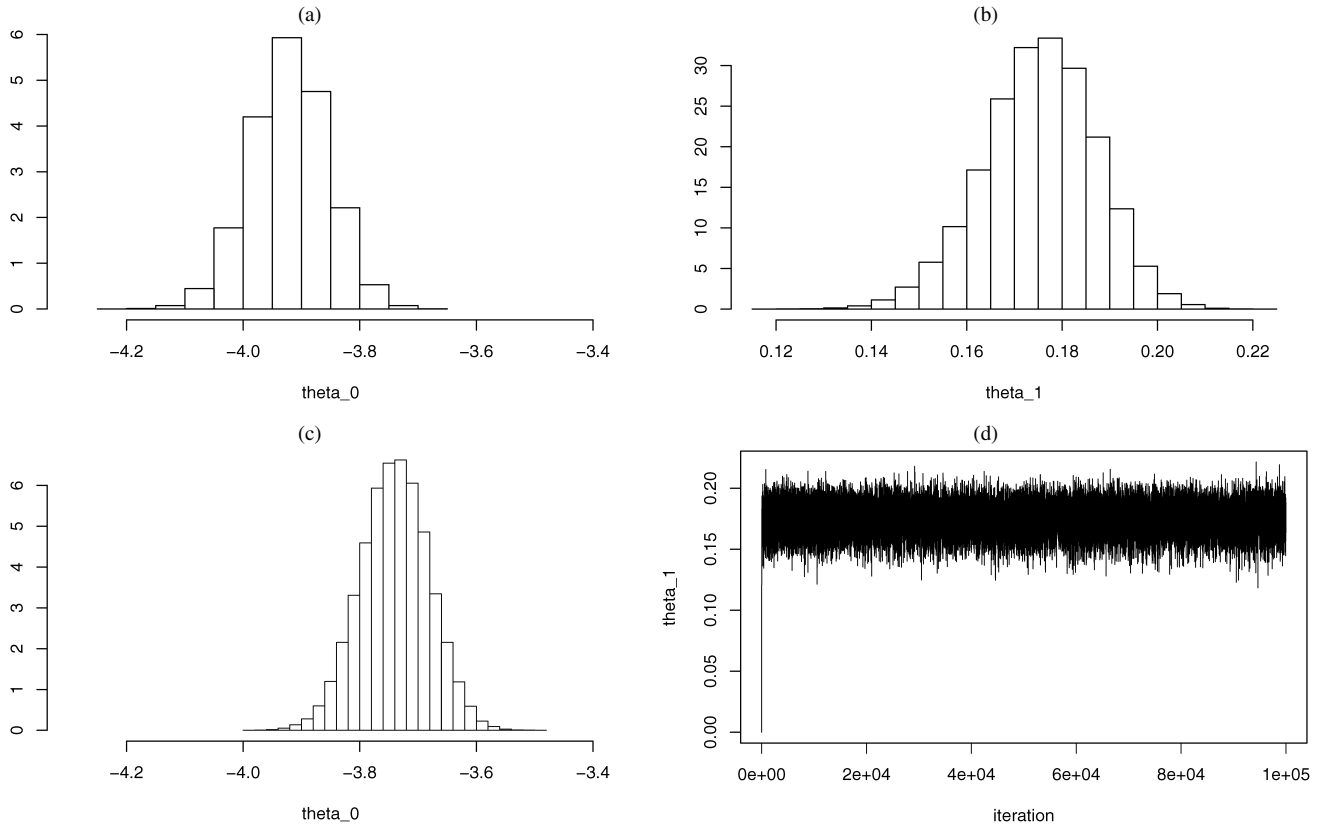

Figure 2. Posterior distribution of (a) and (c) the intercept θ_0; (b) the spatial-temporal coefficient θ_1 in the turpentine beetle colonization model. The first row is based on the spatial-temporal model (8), and the second row is based on the independence model. Selected trace plot of θ_1 in the spatial-temporal model is shown in (d).

$n = 1{,}000$. The results suggest a positive relationship among *Ips* spp. colonization in the current year and the number of turpentine beetle tubes in the same year at the same site, *Ips* spp. colonization in the previous year at the neighboring sites (excluding the same site), and *Ips* spp. colonization in the current year at the neighboring sites (excluding the same site), up to the second-order neighbors. In other words, the more turpentine beetles there are on a tree, the more likely that the tree will be colonized by *Ips* spp. Thus there is strong evidence that turpentine beetles predispose trees to colonization by *Ips* spp. Moreover, there is clear spatial and temporal dependence in the *Ips* spp. colonization. The more trees in the neighborhood that were colonized by *Ips* spp. in the previous year, the more likely that the tree is colonized by *Ips* spp. in the current year. Similarly, the more trees in the neighborhood that are colonized by *Ips* spp. in the current year, the more likely that the tree is colonized by *Ips* spp. in the current year. Here the extent of local temporal dependence is represented by a 1-year lag and that of local spatial dependence is represented by about 2.07 m, the distance between a second-order neighbor and the site of the tree. A concentration of *Ips* spp. attacks in nearby trees may occur for three reasons, which are not mutually exclusive. First, insect brood emerging from a previously colonized tree would preferentially colonize nearby trees. This may occur if, for example, brood adults from late fall overwinter in the duff around the base of their brood tree and then emerge to colonize nearby trees in the spring. Although little is known about the relationships between brood trees and overwintering locations, inclement weather and predators exert substantial mortality on bark beetles engaging in host-seeking behaviors (Berryman 1979). Second, localized attacks may occur when high numbers of bark beetles are attracted by aggregation pheromones of a successful attack and begin to attack nearby trees, a phenomena known as "switching" (Geiszler, Gallucci, and Gara 1980). Third, turpentine beetles and/or fungal root pathogens may weaken trees in local neighborhoods, making them more susceptible to attacks and colonizations by *Ips* spp. (Owen 1985). In comparison, Figures 3(e) and 3(f) give the posterior distributions of ψ_0 and ψ_1 under the independence model. Note that without accounting for spatial-temporal dependence, although the relationship between the *Ips* spp. colonization and the number of turpentine beetle tubes in the same year at the same site remains positive, the strength of the relationship appears to be much weaker than the results in the spatial-temporal model. The spread of the posterior distribution is also smaller than that in the spatial-temporal model.

For inference of the parameters $\boldsymbol{\varphi}$ in the tree condition model, Figures 4(a)–4(d) give the posterior distributions based on an MCMC run length of 100,000 with a burn-in length of 1,000. The results suggest that there is no evidence of a direct relationship between a tree's condition and the number of its turpentine beetle tubes, but there is a strong positive relationship between *Ips* spp. colonization and subsequent tree death. That is, the number of turpentine beetles does not directly influence the mortality of tree, but there is a very large increase in the

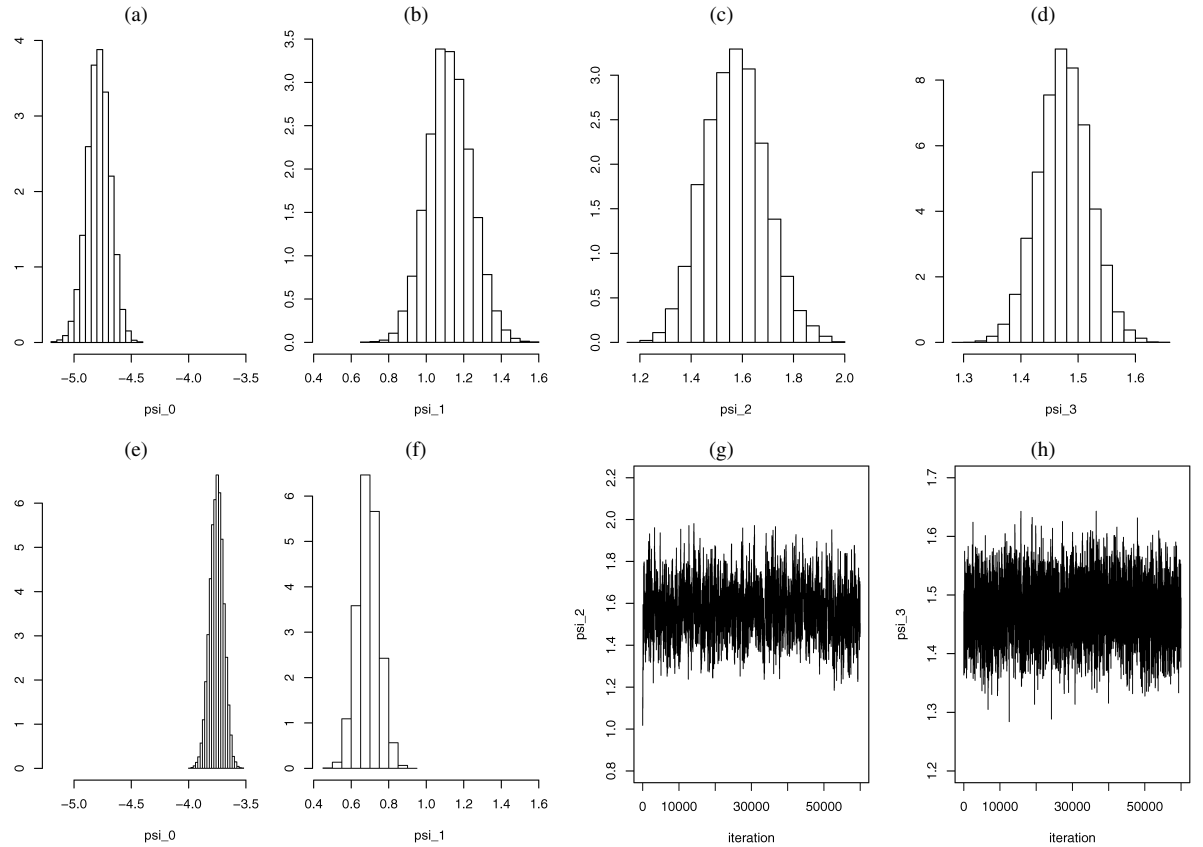

Figure 3. Posterior distribution of (a) and (e) the intercept ψ_0; (b) and (f) the turpentine beetle coefficient ψ_1; (c) the spatial-temporal coefficient for previous time ψ_2; (d) the spatial-temporal coefficient for current time ψ_3 in the *Ips* spp. colonization model. The first row is based on the spatial-temporal model (12), and the second row is based on the independence model. Selected trace plots of ψ_2 and ψ_3 in the spatial-temporal model are shown in (g) and (h).

probability that a tree dies after colonized by *Ips* spp. in the same year. This is not surprising, because trees may survive colonization of the root collar by turpentine beetles for more than 1 year. However, *Ips* spp. use aggregation pheromones to attract high numbers of conspecifics that quickly colonize all available subcortical tissue. The water-conducting tissues are mined by the developing larvae, and the tree dies soon thereafter. Furthermore, it appears necessary to account for the spatial-temporal dependence among the tree conditions. Again in comparison, Figures 4(e)–4(g) give the posterior distributions of φ_0, φ_1, and φ_2 under the independence model. The difference in the results between the spatial-temporal model and the independence model is not as pronounced as in the case of *Ips* spp., although with the independence model, the relationship between tree mortality and *Ips* spp. colonization is slightly stronger, with somewhat less variation in the posterior distribution of φ_2.

5.2 Empirical and Predictive Rates of Mortality and *Ips* spp. Colonization

In this and the next section we check important aspects of the model that correspond to the ecological questions of interest, particularly the relationships among turpentine beetle colonization, *Ips* spp. colonization, and tree conditions (see Sec. 1). This model checking is based on posterior predictive distributions obtained by a Monte Carlo sample $(\mathbf{x}^{(s)}, \mathbf{u}^{(s)}, \mathbf{z}^{(s)})$, $s = 1, \ldots, S$, where the Monte Carlo sample size is chosen to be $S = 100$. More precisely, because inference is performed conditional on $\mathbf{e}$, given a posterior simulation $(\boldsymbol{\theta}^{(s)}, \boldsymbol{\psi}^{(s)}, \boldsymbol{\varphi}^{(s)})$, we simulate "new data" $(\mathbf{x}^{(s)}, \mathbf{u}^{(s)}, \mathbf{z}^{(s)})$ from the conditional distribution of $\mathbf{d}$ given $\mathbf{e}$ as specified in (4) and (5). We do this using the sequential model construction in Section 3, where simulation of $\mathbf{x}_t$ and $\mathbf{z}_t$ given their relevant past is straightforward (see Secs. 3.3 and 3.5), whereas we use perfect simulation for $\mathbf{y}_t$ given the relevant past (see Sec. 3.4). Note that $\mathbf{x}_0^{(s)} = \mathbf{x}_0$, $\mathbf{y}_0^{(s)} = \mathbf{y}_0$, and $\mathbf{z}_{-1}^{(s)} = \mathbf{z}_{-1}$. The samples $(\boldsymbol{\theta}^{(s)}, \boldsymbol{\psi}^{(s)}, \boldsymbol{\varphi}^{(s)})$, $s = 1, \ldots, S$, are chosen such that they are effectively independent posterior simulations. Moreover, we let $(\mathbf{x}^{(0)}, \mathbf{y}^{(0)}, \mathbf{z}^{(0)})$ denote the data. For comparison, we also simulate "new data" from the independence models, with the model parameters drawn from the corresponding posterior distributions.

In this section we consider the posterior predictive distribution of various statistics related to mortality rates of trees and rates of *Ips* spp. colonization. First, define

$$\mathcal{I}_{0,0} = \{i : z_{-1,i} = 0, x_{0,i} = 0, u_{0,i} = 0\},$$

$$\mathcal{I}_{0,1} = \{i : z_{-1,i} = 0, x_{0,i} = 0, u_{0,i} = 1\},$$

$$\mathcal{I}_{1,0} = \{i : z_{-1,i} = 0, x_{0,i} > 0, u_{0,i} = 0\},$$

$$\mathcal{I}_{1,1} = \{i : z_{-1,i} = 0, x_{0,i} > 0, u_{0,i} = 1\},$$

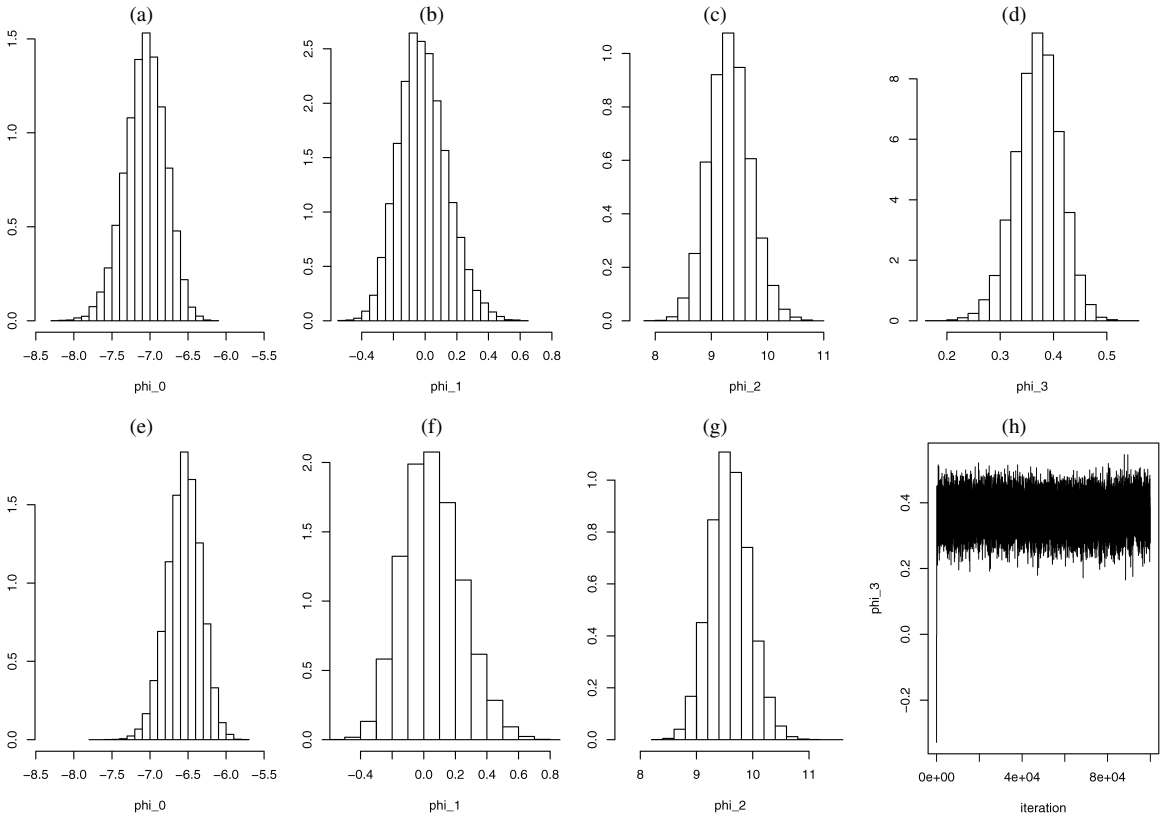

Figure 4. Posterior distribution of (a) and (e) the intercept φ_0; (b) and (f) the turpentine beetle coefficient φ_1; (c) the *Ips* spp. coefficient φ_2; (d) the spatial-temporal coefficient φ_3 in the tree condition model. The first row is based on the spatial-temporal model (15), and the second row is based on the independence model. A selected trace plot of φ_3 in the spatial-temporal model is shown in (h).

and

$$p_{k,l}^{(s)}(t) = \frac{1}{|\mathcal{I}_{k,l}|} \sum_{i \in \mathcal{I}_{k,l}} \mathbf{1}\big[z_{t,i}^{(s)} = 1\big],$$

$$s = 0, \ldots, S, t = 0, \ldots, 5, k, l = 0, 1,$$

where $|A|$ denotes the cardinality of a finite set A. Then $p_{0,0}^{(0)}(t)$ is the observed tree mortality rate of trees that were alive at time -1 and had no bark beetle colonization by time 0, $p_{0,1}^{(0)}(t)$ is the observed mortality rate of trees colonized by *Ips* spp., $p_{1,0}^{(0)}(t)$ is the observed mortality rate of trees colonized by turpentine beetles, and $p_{1,1}^{(0)}(t)$ is the observed mortality rate of trees colonized by both turpentine beetles and *Ips* spp.

Figures 5(a)–5(c) show for each value of $(k, l) = (0, 0)$, $(0, 1)$, $(1, 0)$ and $t = 0, \ldots, 5$ the observed mortality rate $p_{k,l}^{(0)}(t)$ and the 2.5th, 50th, and 97.5th percentiles of the posterior predictive distribution obtained from $p_{k,l}^{(s)}(t)$, $s = 1, \ldots, S$. Furthermore, for the case of $(k, l) = (1, 1)$ (not shown in Fig. 5), the 2.5th, 50th, and 97.5th percentiles for the mortality rates are .50, 1.00, and 1.00 for all times $t = 0, \ldots, 5$, with the corresponding observed values being all 1.00. For all values of (k, l), the observed rates lie in the centers of the corresponding predictive distributions. Thus overall, there is no evidence against our spatial-temporal models. Compared with $p_{0,0}^{(0)}(t)$, which may be interpreted as a kind of observed baseline mortality rate, $p_{0,1}^{(0)}(t)$ increased greatly, with the large increase occurring in the same year as *Ips* spp. colonization; $p_{1,0}^{(0)}(t)$ increased at time 1, with the increase levelling off at time 2; and $p_{1,1}^{(0)}(t)$ was nearly 100% within the same year of the colonization. The predictive distributions show a similar behavior. The fact that tree deaths occurred in both the first and second years after turpentine beetle colonization provides further evidence that turpentine beetles predispose a tree to death rather than killing a tree directly. The result here also supports the theory that *Ips* spp., unlike turpentine beetles, are the ultimate mortality agents of red pines.

In contrast, Figures 5(d)–5(f) are drawn in the same way but are based on the independence models. In the case of $(k, l) = (1, 0)$ [Fig. 5(c) and 5(f)], we note that the 95% prediction intervals for tree mortality are substantially lower and wider in the independence models than the spatial-temporal models. Furthermore, the observed mortality rate is completely outside the 95% predictive interval at time $t = 1$ and is barely within the 95% intervals at time $t = 2$, indicating a misfit of the independence models in representing the effect of turpentine beetles on tree mortality at two critical times, $t = 1, 2$, after turpentine beetle colonization.

Next, let

$$\mathcal{I}_k = \{i : z_{-1,i} = 0, x_{0,i} = k\}, \qquad k = 0, 1,$$

denote the collection of sites at which a tree was alive at time -1 and was $(k = 1)$ or was not $(k = 0)$ colonized by tur-

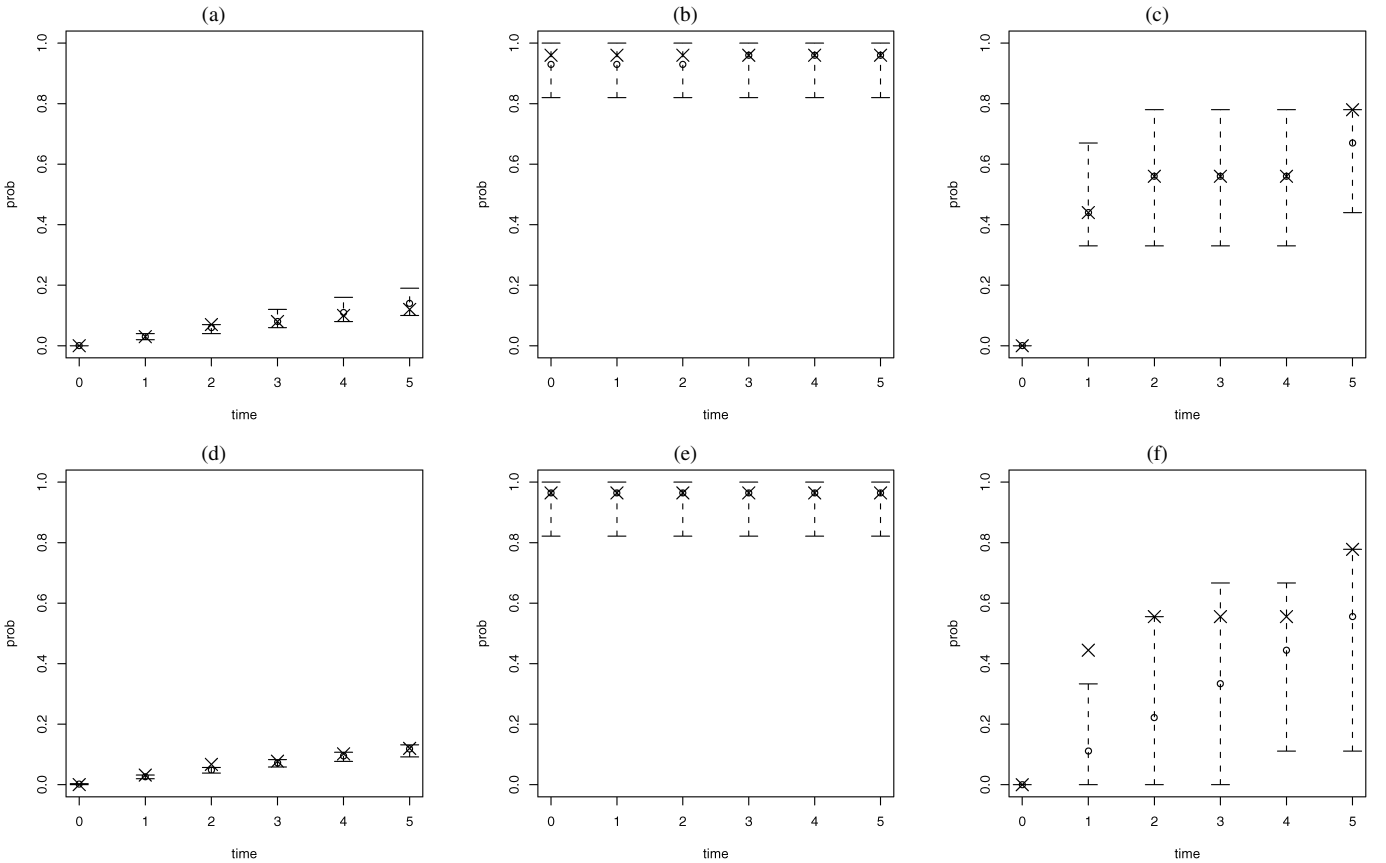

Figure 5. Central 95% prediction intervals for the tree mortality rates over time $t = 0, \ldots, 5$ among those trees that were alive at $t = -1$ and were not colonized ($x_{i,0} = 0, u_{i,0} = 0$) [(a) and (d)]; and colonized by *Ips* spp. ($x_{i,0} = 0, u_{i,0} = 1$) [(b) and (e)]; and colonized by turpentine beetles ($x_{i,0} > 0, u_{i,0} = 0$) at $t = 0$ [(c) and (f)]. The first row is based on the spatial-temporal models, and the second row is based on the independence models. The medians of the posterior predictive distributions are indicated by circles, and the observed tree mortality rates are indicated by crosses.

pentine beetles by time 0, and let

$$p_k^{(s)}(t) = \frac{1}{|\mathcal{I}_k|} \sum_{i \in \mathcal{I}_k} \mathbf{1}\big[u_{t,i}^{(s)} = 1\big],$$

$$s = 0, \ldots, S, t = 0, \ldots, 5, k = 0, 1.$$

Then $p_k^{(0)}(t)$ is the observed rate of *Ips* spp. colonization of a tree from $\mathcal{I}_k$ by time $t = 0, \ldots, 5$. Figure 6 is similar to Figure 5 but concerns $p_k^{(s)}(t)$ for $k = 0, 1$ and $t = 0, \ldots, 5$. Again, there is no evidence against the spatial-temporal models. Compared with $p_0^{(0)}(t)$, the rates of *Ips* spp. colonization $p_1^{(0)}(t)$ were much higher and leveled off after 2–3 years, supporting the theory that turpentine beetles predispose the trees to subsequent colonization and killing by *Ips* spp.

Again in contrast, in the case of $x_{i,0} > 0$ [Figs. 6(b) and 6(d)], we note that the 95% prediction intervals for tree mortality are lower and wider in the independence models than in the spatial-temporal models. The observed mortality rate is completely outside the 95% predictive interval at time $t = 1$ and is barely within the 95% intervals at time $t = 2$, again indicating a poor fit of the independence models.

5.3 Checking Further Aspects of the Model

To check whether the model captures the relationships between turpentine beetle colonization and *Ips* spp. colonization and between colonization of *Ips* spp. and tree mortality, we consider

$$r_{x,u}^{(s)} = \sum_{t=1}^{5} \sum_{i} \big(x_{t,i}^{(s)} - x_{t-1,i}^{(s)}\big) u_{t,i}^{(s)},$$

$$r_{u,z}^{(s)} = \sum_{t=1}^{5} \sum_{i} u_{t,i}^{(s)} z_{t,i}^{(s)}, \quad s = 0, \ldots, S.$$

Here $r_{x,u}^{(0)}$ summarizes the observed relationship between new colonization of turpentine beetles and new colonization of *Ips* spp. in the same year and at the same site, and $r_{u,z}^{(0)}$ summarizes the observed occurrences of *Ips* spp. colonization involved in tree mortality. Furthermore, for spatial dependence structure, we consider

$$v_{x,x}^{(s)}(\delta) = \sum_{i,j\,:\,d(i,j) \in N(\delta)} \mathbf{1}\big[x_{5,i}^{(s)} > 0, x_{5,j}^{(s)} > 0\big],$$

$$s = 0, \ldots, S, \delta > 0,$$

$$v_{y,y}^{(s)}(\delta) = \sum_{i,j : d(i,j) \in N(\delta)} \mathbf{1}\big[y_{5,i}^{(s)} > 0, y_{5,j}^{(s)} > 0\big],$$

$$s = 0, \ldots, S, \delta > 0,$$

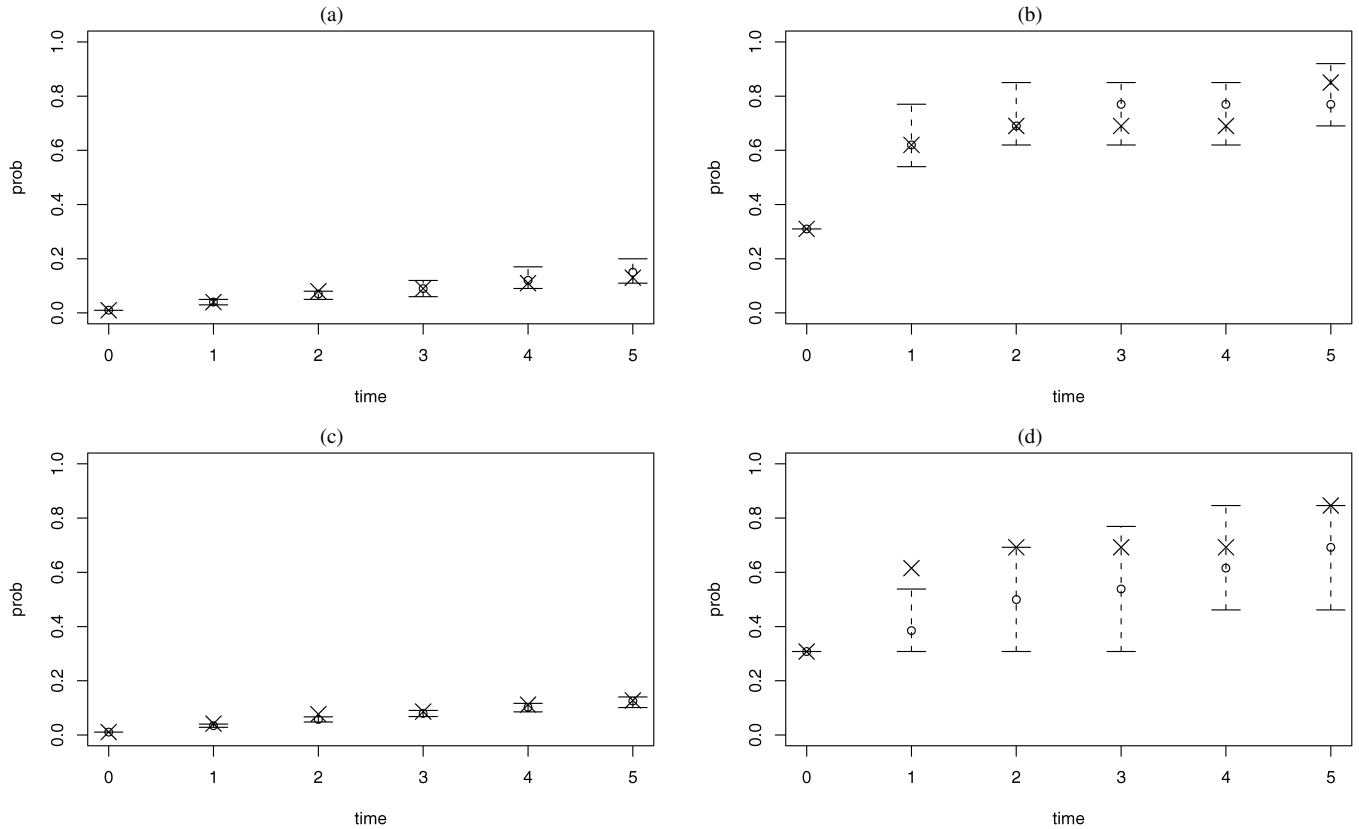

Figure 6. Central 95% prediction intervals for the rate of *Ips* spp. colonization over time $t = 0, \ldots, 5$ among those trees that were alive at $t = -1$ and were not colonized by turpentine beetles ($x_{i,0} = 0$) [(a) and (c)] and colonized by turpentine beetles ($x_{i,0} > 0$) at $t = 0$ [(b) and (d)]. The first row is based on the spatial-temporal models, and the second row is based on the independence models. The medians of the posterior predictive distributions are indicated by circles, and the observed rates of *Ips* spp. colonization are indicated by crosses.

and

$$v_{z,z}^{(s)}(\delta) = \sum_{i,j:d(i,j)\in N(\delta)} \mathbf{1}\big[z_{5,i}^{(s)} = 1, z_{5,j}^{(s)} = 1\big],$$

$$s = 0, \ldots, S, \delta > 0,$$

where $d(i, j)$ denotes the Euclidean distance between sites i and j and $N(\delta) = (\delta - 1, \delta]$ is a half-open interval. That is, $v_{x,x}^{(0)}(\delta)$ $[v_{y,y}^{(0)}(\delta), v_{z,z}^{(0)}(\delta)]$ represents the observed spatial relationship between turpentine beetle colonization (*Ips* spp. colonization, tree mortality) at two sites that are at least $\delta - 1$ and at most δ apart in distance. Here we focus on the cumulative effect of all three variables for simplicity. Finally, for the temporal dependence structure, we consider

$$w_x^{(s)}(t) = \frac{1}{N}\sum_{i=1}^{N} \mathbf{1}\big[x_{t,i}^{(s)} = 0\big],$$

$$w_y^{(s)}(t) = \frac{1}{N}\sum_{i=1}^{N} \mathbf{1}\big[y_{t,i}^{(s)} = 0\big],$$

$$w_z^{(s)}(t) = \frac{1}{N}\sum_{i=1}^{N} \mathbf{1}\big[z_{t,i}^{(s)} = 0\big],$$

where $s = 0, \ldots, S$, $t = 0, \ldots, 5$ for $w_x(t)$ and $w_y(t)$; $t = -1, \ldots, 5$ for $w_z(t)$; and $N = 2{,}715$. That is, $w_x^{(0)}(t)$ $(w_y^{(0)}(t), w_z^{(0)}(t))$ is the observed proportion of trees that are not colonized by turpentine beetles (that are not colonized by *Ips* spp., that are alive) by time t.

Figure 7 is similar to Figure 5 but concerns the foregoing statistics. The 2.5th, 50th, and 97.5th percentiles are 14.0, 28.0, and 149.0 for $r_{x,u}^{(s)}$ and 225.0, 314.5, and 409.0 for $r_{u,z}^{(s)}$. Thus, the observed values $r_{x,u}^{(0)} = 58$ and $r_{u,z}^{(0)} = 269$ fall well within the central 95% prediction intervals. In comparison, the 2.5th, 50th, and 97.5th percentiles are 6.0, 13.0, and 21.0 for $r_{x,u}^{(s)}$ and 210.0, 261.7, and 294.2 for $r_{u,z}^{(s)}$. Thus the observed value $r_{x,u}^{(0)} = 58$ is well outside the 95% prediction interval, whereas $r_{u,z}^{(0)} = 269$ falls within the central 95% prediction intervals. This indicates that the independence models appear to be unable to adequately represent the effect of turpentine beetle in relation to *Ips* spp.

Our spatial-temporal models also adequately represent the spatial dependence for turpentine beetle colonization at all lag distances [see $v_{x,x}^{(s)}(\delta)$ in Fig. 7(a)]. For *Ips* spp. colonization and tree condition [see $v_{y,y}^{(s)}(\delta)$ and $v_{z,z}^{(s)}(\delta)$ in Figs. 7(b) and 7(c)], the spatial dependence is well represented by the model when the lag distances are small. The observed values tend to be larger than what the model predicts, which may be a result of the large cluster of trees that were colonized by *Ips* spp. and/or were dead in the southeastern part of the plantation. The independence models clearly fail to represent the spatial dependence for both *Ips* spp. [shown in Fig. 7(e)] and tree con-

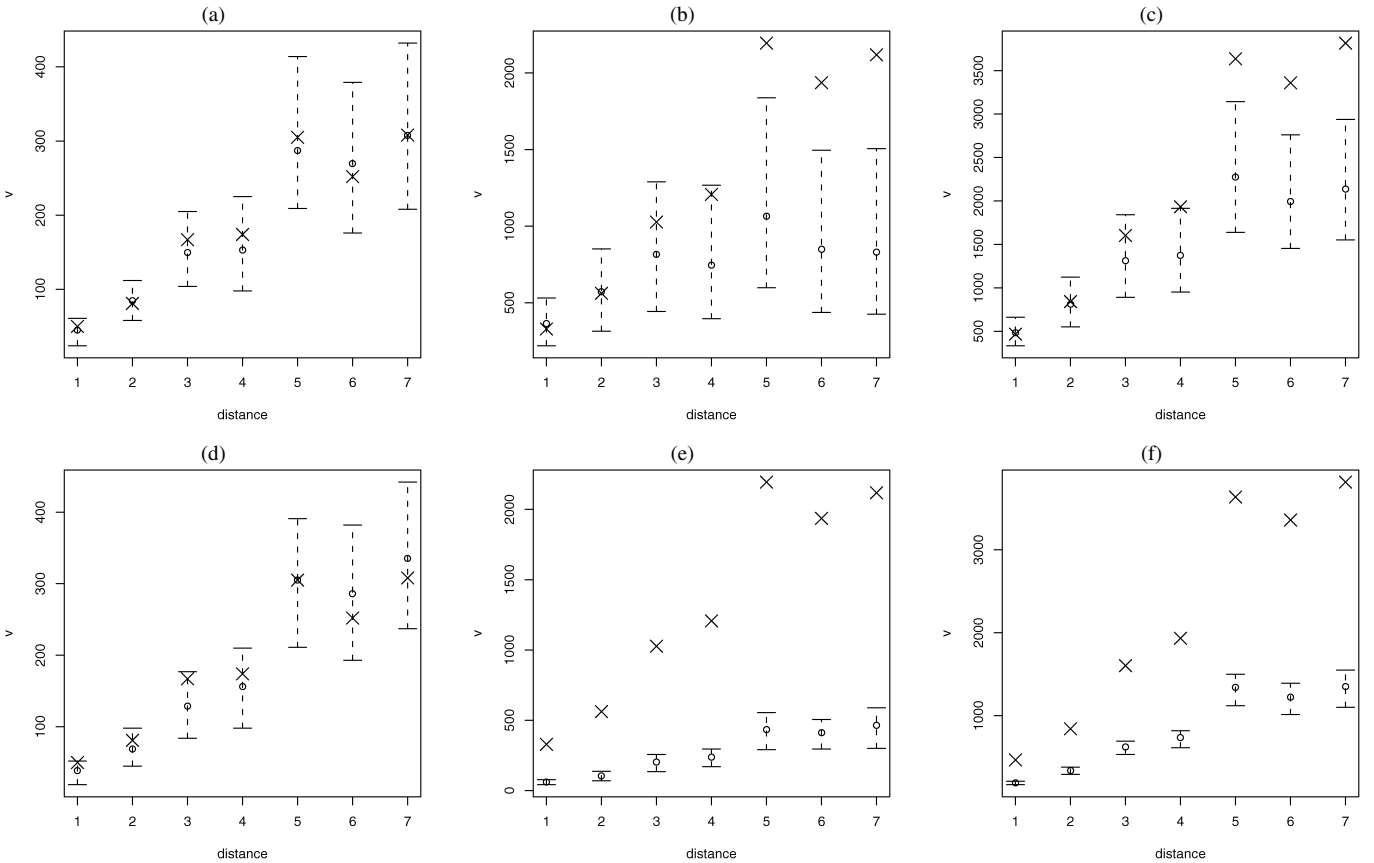

Figure 7. Central 95% prediction intervals for turpentine beetle spatial pattern $v^{(s)}_{x,x}(\delta)$ [(a) and (d)]; *Ips* spp. spatial pattern $v^{(s)}_{u,u}(\delta)$ [(b) and (e)]; and tree mortality spatial pattern $v^{(s)}_{z,z}(\delta)$ [(c) and (f)] as part of model checking. The first row is based on the spatial-temporal models, and the second row is based on the independence models. The medians of the posterior predictive distributions are indicated by circles, and the observed values are indicated by crosses.

dition [shown in Fig. 7(f)], because the observed values are well outside the 95% prediction intervals at all spatial lags.

Furthermore, our spatial-temporal models adequately represent the temporal dependence for *Ips* spp. colonization and tree condition at all time points [see $w^{(s)}_y(t)$ and $w^{(s)}_z(t)$ in Figs. 8(b) and 8(c)]. For turpentine beetle colonization [see $w^{(s)}_x(t)$ in Fig. 8(a)], the observed values tend to be slightly larger than what the model predicts, for reasons that are unclear to us. The results with the independence models [Figs. 8(d)–8(f)] are somewhat similar to those for the spatial-temporal models, although the 95% prediction intervals appear much narrower and the observed values fall outside the prediction intervals at time $t = 3$ for both *Ips* spp. and tree condition.

6. CONCLUDING REMARKS

In this article we have examined the effect of two bark beetle groups on the mortality of red pine trees in a Wisconsin plantation. We have constructed spatial-temporal statistical models to quantify the relationships among turpentine beetle colonization, *Ips* spp. colonization, and mortality of red pine trees while accounting for correlation across space and over time. For statistical inference, we have adopted a Bayesian hierarchical model and devised MCMC algorithms for obtaining the posterior distributions of model parameters. The data analysis in Section 5 suggests that turpentine beetle colonization is associated with higher likelihood of *Ips* spp. colonization and that *Ips* spp. colonization is associated with a greater likelihood of red pine tree mortality, whereas there is no direct association between turpentine beetle colonization and red pine tree mortality. There is strong evidence that turpentine beetle colonization does not kill a red pine tree directly, but rather predisposes the tree to subsequent colonization by *Ips* spp. The evidence is also strong that *Ips* spp. are the ultimate mortality agents of red pine trees.

Based on the results in Sections 5.2 and 5.3, our impression is that the spatial-temporal model in Section 3 has adequately captured the relationships among the three variables turpentine beetle colonization, *Ips* spp. colonization, and tree condition. Moreover, our spatial-temporal models have often, although not always, adequately represented the spatial and temporal structure. This is in contrast to the model-fitting results using independence models, where spatial-temporal dependence is ignored. There we have found that, although the more obvious relationship between *Ips* spp. and tree mortality still can be captured, the more subtle relationship between turpentine beetles and *Ips* spp. can be misrepresented, highlighting the importance of accounting for spatial-temporal dependence.

On one hand, the modeling approach here is of general utility to systems in which interactions among several species affect overall dynamics, but likewise generate spatial-temporal patterns that can complicate dissection of underlying processes.

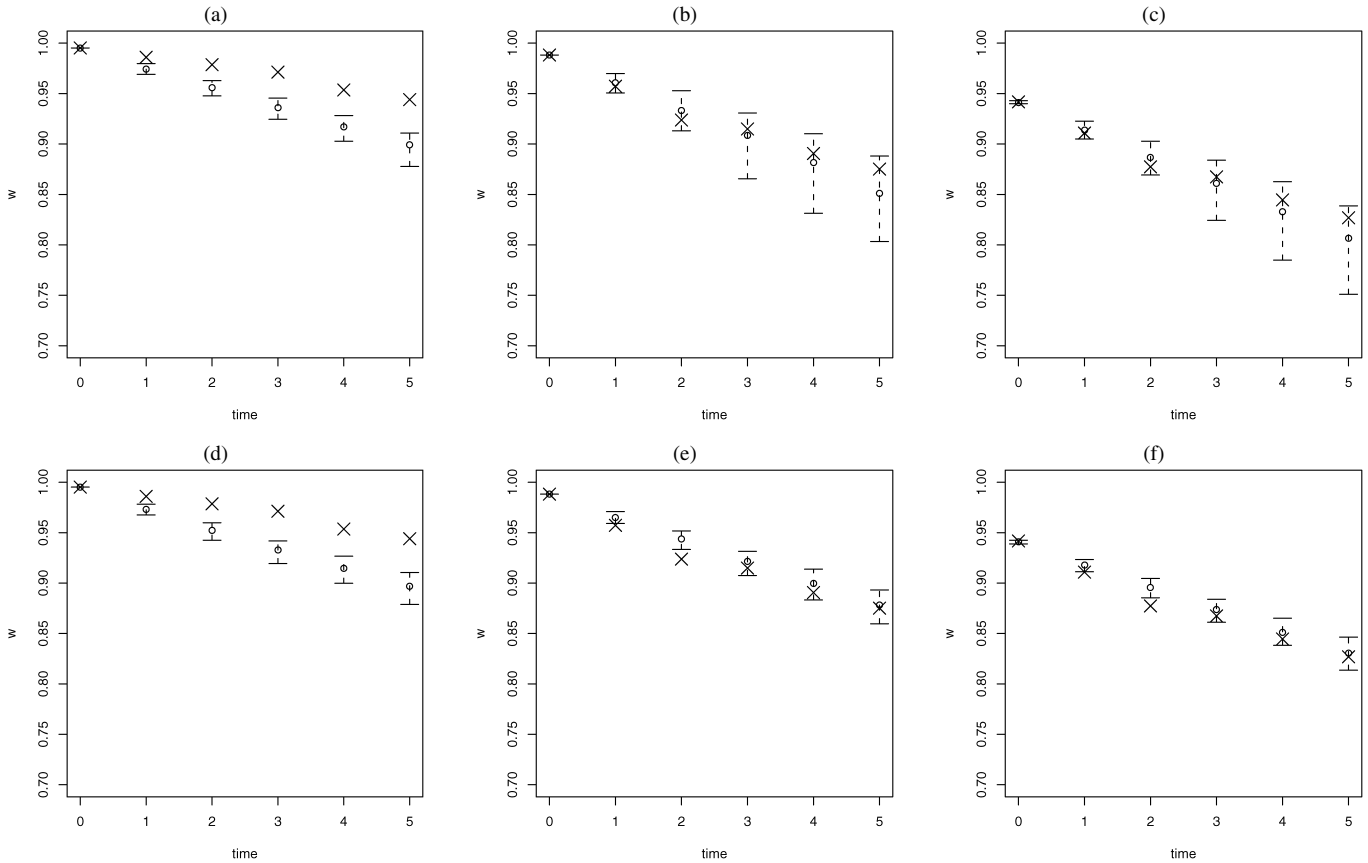

Figure 8. Central 95% prediction intervals for turpentine beetle temporal pattern $w_x^{(s)}(t)$ [(a) and (d)]; *Ips* spp. temporal pattern $w_u^{(s)}(t)$, [(b) and (e)]; tree mortality temporal pattern $w_z^{(s)}(t)$ [(c) and (f)] as part of model checking. The first row is based on the spatial-temporal models, and the second row is based on the independence models. The medians of the posterior predictive distributions are indicated by circles, and the corresponding observed values are indicated by crosses.

Such systems are quite likely common in forest ecosystems. Using this approach can help managers predict insect and pathogen dynamics as well as direct preventive and remedial measures against inciting rather than merely ultimate agents affecting forest health. Although unexplored, the statistical approach taken here can be readily extended to include additional covariates that are spatially indexed and to consider asymmetric neighborhood structures that account for potential anisotropy. We also note that the Bayesian inference presented here could be readily extended for prediction. For instance, it is straightforward to predict bark beetle colonization and tree mortality using posterior predictive distributions, in a manner similar to the approach taken in Section 5.2. That is, new data at future time points can be simulated according to the spatial-temporal models given a posterior simulation of the model parameters. This approach to prediction is often preferred over the frequentist approach, because uncertainty in parameter estimates and variables both can be accounted for. Moreover, because of the built-in connections among the multiple response variables, the prediction can be performed on all of the variables of interest simultaneously, which might be considered an added advantage of the current modeling approach.

On the other hand, several aspects of our modeling approach call for further investigation in the future. These aspects share a common theme of balancing model complexity and computational feasibility. Because of the large amount of computation involved in path sampling combined with perfect simulation, we have relied on our scientific understanding of the system under study, rather than purely on data, to guide our choices of models. For example, we have chosen to model spatial dependence within the same year only for the *Ips* spp. colonization, but not for turpentine beetle colonization or tree condition. We also have chosen a smaller neighborhood (up to the second-order neighbors) for the *Ips* spp. model compared with a larger neighborhood (up to the fifth-order neighbors) for the turpentine beetle and tree condition models. Despite the fact that our model checking has indicated a satisfactory fit of our current models, an autologistic model with the larger neighborhood is applicable in theory for tree condition, whereas auto-Poisson models in a Winsorized version could be extended from the work of Kaiser and Cressie (1997) for turpentine beetle colonization. Similarly, more complex models that account for spatially varying rates of dispersal proposed by Wikle and Hooten (2006) also would be very interesting. However, we expect a substantial increase in computational time as a result of added complexity of the models combined with a large number of trees in this study. It would be extremely helpful to develop efficient computational algorithms for these more complicated models, including our spatial-temporal autologistic models, so that they are more feasible for large data sets. (See Zheng and Zhu 2008 for a comparison of several other

approaches to the inference of spatial-temporal autologistic regression models.) One direction for future research is to extend an exact computational method developed by Møller, Pettitt, Reeves, and Berthelsen (2006) and applied by Berthelsen and Møller (2006). The novelty of this technique lies in the introduction of an auxiliary variable in a Metropolis–Hastings algorithm and the choice of proposal distribution so that no approximation of the normalizing constant is needed. We have chosen to use an approximation of the ratio of normalizing constants here, because the current exact method is not straightforward to use. However, it may provide a method of constructing other and possibly more efficient MCMC algorithms.

APPENDIX: PROPRIETY OF THE POSTERIORS

From a practical standpoint, we would expect our MCMC runs to diverge if an improper posterior distribution had been specified. From a theoretical standpoint, because the three likelihood functions in (17) are log-concave, propriety of the posteriors with uniform improper priors is equivalent to the existence of the MLE based on $L^{(1)}(\boldsymbol{\theta})$, $L^{(2)}(\boldsymbol{\psi})$, and $L^{(3)}(\boldsymbol{\varphi})$. This can be established as sketched here.

The likelihood functions $L^{(1)}(\boldsymbol{\theta})$, $L^{(2)}(\boldsymbol{\psi})$, and $L^{(3)}(\boldsymbol{\varphi})$ in (9), (13), and (16) are products of log-concave functions $L_t^{(1)}(\boldsymbol{\theta})$, $L_t^{(2)}(\boldsymbol{\psi})$, and $L_t^{(3)}(\boldsymbol{\varphi})$. Therefore, to verify the existence of the MLE based on $L^{(1)}(\boldsymbol{\theta})$, $L^{(2)}(\boldsymbol{\psi})$, and $L^{(3)}(\boldsymbol{\varphi})$, it suffices for each $t = 1, \ldots, 5$ to verify the existence of the MLE based on $L_t^{(1)}(\boldsymbol{\theta})$, $L_t^{(2)}(\boldsymbol{\psi})$, and $L_t^{(3)}(\boldsymbol{\varphi})$. This can be easily checked in the cases of the Poisson regression $L_t^{(1)}(\boldsymbol{\theta})$ based on the data $\mathbf{x}_t$ and the logistic regression $L^{(3)}(\boldsymbol{\varphi})$ based on the data $\mathbf{z}_t$, either by theoretical results (Barndorff-Nielsen 1978; Jacobsen 1989) or using software for generalized linear models (see also Gelman, Carlin, Stern, and Rubin 2004). Moreover, by (13), $L_t^{(2)}(\boldsymbol{\psi})$ is of regular exponential family form with canonical statistic

$$s_t^{(2)}(\mathbf{u}_t) = \sum_{i: y_{t-1,i} = z_{t-1,i} = 0} \Bigg(u_{t,i}, x_{t,i} u_{t,i}, \sum_{j \in N_i^y} u_{t-1,j} u_{t,i}, \sum_{j: j \in N_i^y} u_{t,i} u_{t,j} \Bigg).$$

Consequently, by a well-known result from exponential family theory (Barndorff-Nielsen 1978), the MLE of $\boldsymbol{\psi}$ based on the data $\mathbf{u}_t$ exists if $s_t^{(2)}(\mathbf{u}_t)$ belongs to the interior of the convex hull of its support. Checking this condition seems less straightforward, so, alternatively, MCMC methods for finding the MLE may be applied (Geyer and Thompson 1992).

[Received January 2006. Revised March 2007.]

REFERENCES

Auclair, A. N. D. (2005), "Patterns and General Characteristics of Severe Forest Dieback From 1950 to 1995 in the Northeastern United States," *Canadian Journal of Forest Research*, 35, 1342–1355.

Aukema, B. H., Clayton, M. K., and Raffa, K. F. (2005), "Modeling Flight Activity and Population Dynamics of the Pine Engraver, *Ips pini*, in the Great Lakes Region: Effects of Weather and Predators Over Short Time Scales," *Population Ecology*, 47, 61–69.

Barndorff-Nielsen, O. E. (1978), *Information and Exponential Families in Statistical Theory*, Chichester, U.K.: Wiley.

Battles, J. J., and Fahey, T. J. (2000), "Gap Dynamics Following Forest Decline: A Case Study of Red Spruce Forests," *Ecological Applications*, 10, 760–774.

Berryman, A. A. (1979), "Dynamics of Bark Beetle Populations: Analysis of Dispersal and Redistribution," *Entomologique Suisse*, 52, 227–234.

Berthelsen, K. K., and Møller, J. (2006), "Bayesian Analysis of Markov Point Processes," in *Case Studies in Spatial Point Process Modeling*, eds. A. Baddeley, P. Gregori, J. Mateu, R. Stoica, and D. Stoyan, New York: Springer-Verlag, pp. 85–97.

Besag, J. (1974), "Spatial Interaction and the Statistical Analysis of Lattice Systems" (with discussion), *Journal of the Royal Statistical Society*, Ser. B, 36, 192–236.

——— (1975), "Statistical Analysis of Non-Lattice Data," *The Statistician*, 24, 179–195.

Diggle, P., Tawn, J. A., and Moyeed, R. A. (1998), "Model-Based Geostatistics" (with discussion), *Applied Statistics*, 47, 299–350.

Drohan, P. J. (2000), "A Study of Sugar Maple (*Acer saccharum Marsh*) Decline During 1979–1989 in Northern Pennsylvania," unpublished doctoral dissertation, Pennsylvania State University, Dept. of Agronomy.

Erbilgin, N., and Raffa, K. F. (2002), "Association of Declining Red Pine Stands With Reduced Populations of Bark Beetle Predators, Seasonal Increases in Root Colonizing Insects, and Incidence of Root Pathogens," *Forest Ecology and Management*, 164, 221–236.

——— (2003), "Spatial Analysis of Forest Gaps Resulting From Bark Beetle Colonization of Red Pines Experiencing Belowground Herbivory and Infection," *Forest Ecology and Management*, 177, 145–153.

Erbilgin, N., Nordheim, E. V., Aukema, B. H., and Raffa, K. F. (2002), "Population Dynamics of *Ips pini* and *Ips grandicollis* in Red Pine Plantations in Wisconsin: Within- and Between-Year Associations With Predators, Competitors, and Habitat Quality," *Environmental Entomology*, 31, 1043–1051.

Foster, J. (2006), "Bayesian Inference for Poisson and Multinomial Log-Linear Models," working paper, University of Southampton, Dept. of Mathematics.

Geiszler, D. R., Gallucci, V. F., and Gara, R. I. (1980), "Modeling the Dynamics of Mountain Pine Beetle Aggregation in a Lodgepole Pine Stand," *Oecologia*, 46, 244–253.

Gelman, A., and Meng, X. L. (1998), "Simulating Normalizing Constants: From Importance Sampling to Bridge Sampling to Path Sampling," *Statistical Science*, 13, 163–185.

Gelman, A., Carlin, J. B., Stern, H., and Rubin, D. (2004), *Bayesian Data Analysis* (2nd ed.), Boca Raton, FL: Chapman & Hall.

Gelman, A., Meng, X. L., and Stern, H. (1996), "Posterior Predictive Assessment of Model Fitness via Realized Discrepancies" (with discussion), *Statistica Sinica*, 6, 733–807.

Geyer, C. J., and Thompson, E. A. (1992), "Constrained Monte Carlo Maximum Likelihood for Dependent Data" (with discussion), *Journal of the Royal Society of Statistics*, Ser. B, 54, 657–699.

Gumpertz, M. L., Graham, J. M., and Ristaino, J. B. (1997), "Autologistic Model of Spatial Pattern of Phytophthora Epidemic in Bell Pepper: Effects of Soil Variables on Disease Presence," *Journal of Agricultural, Biological, and Environmental Statistics*, 2, 131–156.

Guyon, X. (1995), *Random Fields on a Network: Modeling, Statistics, and Applications*, New York: Springer.

Hogan, J. W., and Tchernis, R. (2004), "Bayesian Factor Analysis for Spatially Correlated Data, With Application to Summarizing Area-Level Material Deprivation From Census Data," *Journal of the American Statistical Association*, 99, 314–324.

Huffer, F. W., and Wu, H. (1998), "Markov Chain Monte Carlo for Autologistic Regression Models With Application to the Distribution of Plant Species," *Biometrics*, 54, 509–524.

Jacobsen, M. (1989), "Existence and Unicity of MLE in Discrete Exponential Family Distributions," *Scandinavian Journal of Statistics*, 16, 335–349.

Kaiser, M. S., and Cressie, N. (1997), "Modeling Poisson Variables With Positive Spatial Dependence," *Statistics and Probability Letters*, 35, 423–432.

Klepzig, K. D., Kruger, E. L., Smalley, E. B., and Raffa, K. F. (1995), "Effects of Biotic and Abiotic Stress on Induced Accumulation of Terpenes and Phenolics in Red Pines Inoculated With Bark Beetle-Vectored Fungus," *Journal of Chemical Ecology*, 21, 601–626.

Klepzig, K. D., Raffa, K. F., and Smalley, E. B. (1991), "Association of Insect-Fungal Complexes With Red Pine Decline in Wisconsin," *Forest Science*, 41, 1119–1139.

Klepzig, K. D., Smalley, E. B., and Raffa, K. F. (1996), "Combined Chemical Defenses Against an Insect–Fungal Complex," *Journal of Chemical Ecology*, 22, 1367–1388.

Møller, J. (1999), "Perfect Simulation of Conditionally Specified Models," *Journal of the Royal Statistical Society*, Ser. B, 61, 251–264.

Møller, J., Pettitt, A. N., Reeves, R. W., and Berthelsen, K. K. (2006), "An Efficient Markov Chain Monte Carlo Method for Distributions With Intractable Normalising Constants," *Biometrika*, 93, 451–458.

Owen, D. R. (1985), "The Role of *Dendroctonus valens* and Its Vectored Fungi in the Mortality of Ponderosa Pine," unpublished doctoral dissertation, University of California Berkeley, Dept. of Entomology.

Propp, J. G., and Wilson, D. B. (1996), "Exact Sampling With Coupled Markov Chains and Applications to Statistical Mechanics," *Random Structures and Algorithms*, 9, 223–252.

Purdon, M., Cienciala, E., Metelka, V., Beranova, J., Hunova, I., and Cerny, M. (2004), "Regional Variation in Forest Health Under Long-Term Air Pollution Mitigated by Lithological Conditions," *Forest Ecology and Management*, 195, 355–371.

Raffa, K. F., and Smalley, E. B. (1995), "Interaction of Pre-Attack and Induced Monoterpene Concentrations in Host Conifer Defense Against Bark Beetle–Fungal Complexes," *Oecologia*, 102, 285–295.

Robert, C., and Casella, G. (2004), *Monte Carlo Statistical Methods* (2nd ed.), New York: Springer.

Roberts, G. O., Gelman, A., and Gilks, W. R. (1997), "Weak Convergence and Optimal Scaling of Random Walk Metropolis Algorithms," *The Annals of Applied Probability*, 7, 110–120.

Wang, F., and Wall, M. M. (2003), "Generalized Common Spatial Factor Model," *Biostatistics*, 4, 569–582.

Wikle, C. K., and Hooten, M. B. (2006), "Hierarchical Bayesian Spatio-Temporal Models for Population Spread," in *Applications of Computational Statistics in the Environmental Sciences: Hierarchical Bayes and MCMC Methods*, eds. J. S. Clark and A. Gelfand, Oxford, U.K.: Oxford University Press, pp. 145–169.

Zheng, Y., and Zhu, J. (2008), "Markov Chain Monte Carlo for Spatial-Temporal Autologistic Regression," *Journal of Computational and Graphical Statistics*, to appear.

Zhu, J., Huang, H.-C., and Wu, J. (2005), "Modeling Spatial-Temporal Binary Data Using Markov Random Fields," *Journal of Agricultural, Biological, and Environmental Statistics*, 10, 212–225.